Nonlinear model reduction for wave energy systems: a moment-matching-based approach

Nonlinear Dynamics manuscript No.
(will be inserted by the editor)

Nonlinear model reduction for wave energy systems

A moment-matching-based approach

Nicolás Faedo · Francisco J. Dores Piuma · Giuseppe Giorgi · John V. Ringwood

Received: – / Accepted: –

Abstract Wave energy converters (WECs) inherently require appropriate control system technology to ensure maximum energy absorption from ocean waves, consequently reducing the associated levelised cost of energy and facilitating their successful commercialisation. Regardless of the control strategy, the definition of the control problem itself depends upon the specification of a suitable WEC model. Not only is the structure of the model relevant for the definition of the control problem, but also its associated complexity: given that the control law must be computed in real-time, there is a limit to the computational complexity of the WEC model employed in the control design procedure, while there is also a limit to the (analytical) complexity of mathematical models for which a control solution can be efficiently found. This paper presents a *systematic* nonlinear model reduction by *moment-matching* framework for WEC systems, capable of providing control-oriented WEC models tailored for the control application, which inherently preserves steady-state response characteristics. Existence and uniqueness of the associated nonlinear moment for WECs is proved in this paper, for a general class of systems. Given that the definition of nonlinear moments depends upon the solution of a nonlinear partial differential equation, an approximation framework for the computation of the nonlinear moment is proposed, tailored for the WEC application. Finally, the use and capabilities of the framework are illustrated by means of case studies, using different WEC systems, under a variety of wave conditions.

Keywords Nonlinear model reduction, Moment-matching, Wave energy conversion, Nonlinear hydrodynamics

Nicolás Faedo (*corresponding author*) · John V. Ringwood
Centre for Ocean Energy Research (COER), Department of Electronic Engineering, Maynooth University, Kildare, Ireland
E-mail: nicolas.faedo@mu.ie

Francisco J. Dores Piuma
Departamento de Ciencia y Tecnología, Universidad Nacional de Quilmes, Bernal, Argentina

Giuseppe Giorgi
Department of Mechanical and Aerospace Engineering, Politecnico di Torino, Turin, Italy

1 Introduction

Control system technology can impact many aspects of wave energy converters (WECs) design and operation, including device sizing and configuration, maximising energy extraction from waves, and optimising energy conversion in the power take-off (PTO) actuator system [23,33]. To be precise, the central problem in WEC control is to find a technically feasible way to 'act' on the device (via the PTO system), so that energy absorption from waves is maximised while minimising the risk of component damage. It is already clear that control technology can enhance WECs performance in a wide range of sea conditions, hence substantially reducing the associated levelised cost of energy (LCoE), constituting a fundamental stepping stone towards successful commercialisation of WEC technology [34].

Regardless of the solution method selected to compute this energy-maximising *optimal* control law, the definition of the control problem itself depends upon[1] the specification of a suitable WEC model Σ. Not only

[1] Though rare due to the inherent complexity behind the energy-maximising control objective for WECs, we note that model-free control techniques also exists within the wave energy control literature. The interested reader is referred to, for instance, [15,39].

is the structure of the model relevant for the definition of the control problem, but also its associated complexity: given that the energy-maximising control law *must* be computed in *real-time*, there is clearly a limit to the computational complexity of the WEC model employed in the control design procedure, while there is also a limit to the (analytical) complexity of mathematical models for which a globally optimal control solution can be efficiently found, or even whether it exists (*i.e.* for which the control problem is *well-posed*) [8,12]. For linear systems, complexity is often understood simply in terms of the dimension (order) of the system. For nonlinear systems, this dimensional argument may be inappropriate, as one also has to take into consideration the complexity of the functions involved in the representation of the system.

That said, even in the most 'simplistic' physical WEC modelling scenario, where linear hydrodynamic conditions[2] are assumed, model reduction techniques are inherently required to provide a control-oriented model: the equation of motion for a WEC under linearity assumptions is non-parametric (due to the presence of a convolution operation associated with *radiation effects* [13]), intrinsically requiring a model reduction procedure, both to alleviate the computational demand of this non-parametric operator, and to express the dynamical equation in a suitable form for control/estimation procedures (often in terms of a state-space representation [9, 40]). Furthermore, any model reduction technique should compute a control-oriented model which inherits the underlying physical properties of the WEC process, so that the approximating structure is effectively representative, including, for instance, internal stability[3]. This is specifically important for WEC control procedures, which often rely on these dynamical properties to guarantee existence and uniqueness of globally optimal solutions [8].

Even though linearity assumptions are often adopted, mostly motivated by their simplicity, the importance of having *nonlinear* control-oriented models has been stressed in recent years [16,17]; WECs are, by their nature, prone to show nonlinear effects[4], since their principal aim, pursued by the optimal control strategy, is to enhance the amplitude of motion to maximise power extraction. In other words, the assumptions under which the linearisation of WEC models is performed are challenged by the controller itself, particularly in relation to assumptions of small movements around the equilibrium position [33]. This may return poor results, both in terms of accuracy of motion prediction, and power production assessment [16,17], which are the key variables involved in any WEC control formulation, directly compromising the role of control technology in maximising energy absorption. The above discussion directly highlights the importance of having *systematic nonlinear model reduction techniques*, which can provide control-oriented nonlinear models, with a level of complexity suitable for the energy-maximising optimal control application. While the availability of nonlinear model reduction techniques would represent an extremely valuable tool, not only for control/estimation procedures, but for a variety of WEC applications (for instance, geometry optimisation and power assessment, among others), there is currently *no literature* addressing this issue within the WEC community, to the best of the authors' knowledge. A number of non-systematic model reduction studies, which produce simpler models by selectively 'ignoring' or 'discarding' nonlinear effects, can be found in, for instance, [30,38]. It is also worth mentioning that some effort has been made recently, in [29], to provide a mathematically consistent *measure* of the impact of each nonlinear effect, and assess which of these significantly affects, for example, power absorption calculations.

Remark 1 If nonlinear effects are considered in control/ state-estimation for WEC applications, only the issue regarding the non-parametric nature of Σ is commonly tackled in the literature, by computing an approximating model for the *linear* radiation dynamics[5], and simply accommodating the nonlinear effects in the corresponding (now parametric) dynamical equation. In other words, there is no nonlinear model reduction process taking place, but rather that the linear system is approximated with a parametric form, hence avoiding the computational complexity and representational drawback of the associated convolution operator.

Motivated by the discussion provided above, and the fundamental requirement of systematic model reduction techniques capable of facilitating accurate control-oriented models, this paper presents a nonlinear model reduction by *moment-matching* framework for WEC systems. Moment-matching methods [1,36], also referred to as *interpolation* methods, are largely based on the

[2] Linear conditions refers to so-called *linear potential flow theory*, see [13].

[3] Within the field of wave energy applications, internal stability is a fundamental requirement of a model representing the physical system not only for control/estimation, but also for motion simulation and power assessment purposes.

[4] The reader is referred to, for instance, [16,27,43] for comprehensive discussions on different sources of nonlinear effects (and associated modelling procedures) in WECs.

[5] Assuming that the non-parametric nature of Σ is only due to linear radiation dynamics. This is not always necessarily the case, since f_{nl} can be potentially non-parametric.

mathematical notion of *moments*. Moments are intrinsically connected to the input-output characteristics of the dynamical system under analysis, and provide a very specific parameterisation of the steady-state output response (provided it exists) of such a system. That said, the model reduction by moment-matching technique consists of the interpolation of the steady-state response of the output of the system to be reduced: a model reduced by moment-matching is such that its steady-state response *exactly matches* the steady-state response of the system to be reduced. A fundamental advantage is that the notion of moments has been defined both for linear and nonlinear systems, by means of a system-theoretic approach, initially proposed in [1]. For linear differential systems, the computation of moments depends upon the solution of a Sylvester equation. For nonlinear differential systems (which is our case of interest), moments arise as the solution of a nonlinear partial differential (invariance) equation.

To that end, the existence and uniqueness of the associated nonlinear moment for WECs is discussed, and ensured in this paper, for the case of wave energy systems. Given that the definition of nonlinear moments depends upon the solution of a nonlinear partial differential equation, an approximation framework for the computation of the nonlinear moment is proposed, tailored for the WEC application. The use and capabilities of the framework are illustrated by means of case studies, using different WEC systems, under a variety of wave conditions.

The remainder of this paper is organised as follows. Notation and conventions utilised in this paper are summarised in Section 1.1. The fundamentals behind nonlinear model reduction by moment-matching are discussed in Section 2, while WEC modelling is briefly addressed in Section 3. A moment-based formulation for the WEC is provided in Section 4, where the existence and uniqueness of the associated moment is discussed and ensured for the case of wave energy systems. An approximation framework for the computation of the nonlinear moment is proposed in Section 5, based on the family of mean weighted residual methods (see, for instance, [14]). Practical aspects and considerations behind this approximation framework are discussed in Section 6. Sections 7 and 8 discuss the case of model reduction for WEC systems under regular, and irregular, wave excitation inputs, respectively. Finally, the main conclusions of this paper are encompassed in Section 9.

1.1 Notation & conventions

Standard notation is considered throughout this manuscript, most of which is defined in this section. If additional notation (not included in this section) is introduced, this is defined in the relevant parts of the paper at the point of introduction.

Sets

$\mathbb{R}^+$ ($\mathbb{R}^-$) denotes the set of non-negative (non-positive) real numbers. $\mathbb{C}^0$ denotes the set of pure-imaginary complex numbers, and $\mathbb{C}_{<0}$ denotes the set of complex numbers with negative real part. The notation $\mathbb{N}_q$ indicates the set of all positive natural numbers up to q, *i.e.* $\mathbb{N}_q = \{1, 2, \dots, q\}$, while $\mathbb{N}_{\geq q}$ is reserved for the set of natural numbers $\{q, q+1, \dots\} \subset \mathbb{N}$. The span of the set $\mathscr{X} = \{x_i\}_{i=1}^k \subset \mathscr{Z}$, where $\mathscr{Z}$ is a vector space over a field $\mathbb{F}$, is denoted as $\text{span}\{\mathscr{X}\}$.

Scalars, vectors and matrices

The symbol 0 stands for any zero element, dimensioned according to the context. The symbol $\mathbb{I}_n$ denotes the identity matrix of the space $\mathbb{C}^{n\times n}$. The notation $\mathbf{1}_{n\times m}$ is used to denote a *Hadamard* identity matrix, *i.e.* a $n \times m$ matrix with all its entries equal to 1. The spectrum of a matrix $A \in \mathbb{R}^{n\times n}$, *i.e.* the set of its eigenvalues, is denoted as $\lambda(A)$. The *Frobenius* norm of a matrix is denoted as $\|A\|_{\text{F}}$. The symbol $\bigoplus$ denotes the direct sum of n (square) matrices, *i.e.* $\bigoplus_{i=1}^n A_i = \text{diag}(A_1, A_2, \dots, A_n)$. The notation $\Re\{z\}$ and $\Im\{z\}$, with $z \in \mathbb{C}$, stands for the *real-part* and the *imaginary-part* of z, respectively. The symbol $e_{ij}^q \in \mathbb{R}^{q\times q}$ denote a matrix with 1 in the ij entry and 0 elsewhere. Likewise, $e_i^q \in \mathbb{R}^q$ denotes a vector with 1 in the i entry and 0 elsewhere.

Functions

Given two functions, $f : \mathscr{Y} \to \mathscr{Z}$ and $g : \mathscr{X} \to \mathscr{Y}$, the composite function $(f \circ g)(x) = f(g(x))$, which maps all $x \in \mathscr{X}$ to $f(g(x)) \in \mathscr{Z}$, is denoted with $f \circ g$. The convolution between two functions f and g, with $\{f, g\} \subset L^2(\mathbb{R})$, over the set $\mathbb{R}$, *i.e.* $\int_{\mathbb{R}} f(\tau)g(t-\tau)d\tau$ is denoted as $f * g$, and where $L^2(\mathbb{R}) = \{f : \mathbb{R} \to \mathbb{R} \mid \int_{\mathbb{R}} |f(\tau)|^2 d\tau < +\infty\}$ is the Hilbert space of square-integrable functions in $\mathbb{R}$. Let f and g be functions in $L^2(\mathcal{T})$, with $\mathcal{T} \subseteq \mathbb{R}$. Then, the standard inner-product between f and g is defined (and denoted) as $\langle f, g\rangle = \int_{\mathcal{T}} f(t)g(t)dt$. Finally, the Fourier transform of a function f (provided it exists), is denoted as $F(\omega)$, $\omega \in \mathbb{R}$.

2 Model reduction by moment-matching: Preliminaries

This section briefly recalls some of the key concepts behind *nonlinear model reduction by moment-matching*

(also often referred to as *moment-based* framework throughout this paper), as developed and discussed in key studies such as, for instance, [1, 36], for nonlinear single-input single-output (SISO) systems. In particular, special emphasis is placed on the formal definition of a *moment*, using a system-theoretic approach[6].

2.1 Definition of moments

Consider a nonlinear, deterministic, finite-dimensional, SISO, continuous-time system, described, for $t \in \mathbb{R}^+$, by the following set of equations[7]

$$\begin{aligned} \dot{x} &= f(x,u), \\ y &= h(x), \end{aligned} \tag{1}$$

with $x(t) \in \mathbb{R}^n$, $u(t) \in \mathbb{R}$, $y(t) \in \mathbb{R}$, and f and h sufficiently smooth mappings defined in the neighborhood of the origin of $\mathbb{R}^n$. Assume system (1) is *minimal*, *i.e.* *observable* and *accessible* (see [36, Chapter 2]), and suppose that $f(0,0) = 0$ and $h(0) = 0$.

Consider now a *signal generator* (sometimes referred to as *exogenous system* [20]) described, for $t \in \mathbb{R}^+$, by the set of differential equations

$$\begin{aligned} \dot{\xi} &= S\xi, \\ u &= L\xi, \end{aligned} \tag{2}$$

with $\xi(t) \in \mathbb{R}^\nu$, $S \in \mathbb{R}^{\nu\times\nu}$ and $L^\intercal \in \mathbb{R}^\nu$, and the interconnected (or *composite*) system

$$\begin{aligned} \dot{\xi} &= S\xi, \\ \dot{x} &= f(x, L\xi), \\ y &= h(x), \end{aligned} \tag{3}$$

Following [36], a relevant set of assumptions is considered to later formalise the definition of nonlinear moments.

Assumption 1 *The triple of matrices $(L, S, \xi(0))$ is minimal.*

Remark 2 The minimality of the triple $(L, S, \xi(0))$ implies *observability* of the pair (S, L) and *excitability* of the pair $(S, \xi(0))$. Excitability refers (with additional technical assumptions, see [26]) to a geometric characterisation of the property that all signals generated by (2) are persistently exciting.

Remark 3 For linear systems, excitability is equivalent to *reachability*, *i.e.* with $\xi(0)$ playing the role of the input matrix, see [26].

Assumption 1 stems from the fact that the signal generator defined in (2) does not have any input. As a matter of fact, given that this signal generator characterises inputs to the system under analysis, *i.e.* system (1), it is rather natural to construct (2) in such a way that all the modes of motion described by the dynamic matrix S are excited, and that the inputs generated are effectively observable.

Assumption 2 *The signal generator (2) is such that $\lambda(S) \subset \mathbb{C}^0$ with simple eigenvalues*[8]*.*

Assumption 2 guarantees that the signal generator (2) generates *bounded* trajectories. Note that this automatically implies that the output signal $u(t)$, *i.e.* the input to system (1), is also bounded.

Remark 4 Both Assumptions 1 and 2 are in line with 'practical' scenarios and, as demonstrated throughout Section 4, can be adopted without any loss of generality for the WEC case. In particular, given that the signal generator characterises the set of inputs to the system under analysis, it is almost natural to guarantee that the modes of motion described by the signal generator (2) are excited (Assumption 1), and that any generated output is bounded (Assumption 2).

We are now ready to introduce the following main lemma.

Lemma 1 [36] *Suppose Assumptions 1 and 2 hold, and that the zero equilibrium of the system (1) is locally exponentially stable in the Lyapunov sense. Then, there exists a unique mapping π, locally*[9] *defined in a neighborhood Ξ of $\xi = 0$, with $\pi(0) = 0$, which is the solution of the partial differential equation*

$$\frac{\partial \pi(\xi)}{\partial \xi} S\xi = f(\pi(\xi), L\xi), \tag{4}$$

for all $\xi \in \Xi$, and the steady-state response of the interconnected system (1)-(2) is $x_{\text{ss}}(t) = \pi(\xi(t))$, for any $x(0)$ and $\xi(0)$ sufficiently small.

Definition 1 Suppose the assumptions of Lemma 1 are fulfilled. The mapping $h \circ \pi$ is the moment of system (1) at the signal generator (2), *i.e.* at (S, L).

Remark 5 Note that the result of Lemma 1, and the notion of moments stated in Definition 1, imply that the moment of system (1) at (S, L) computed along a particular trajectory $\xi(t)$ coincides with the (well-defined) steady-state response of the output of the interconnected system (3), *i.e.* $y_{\text{ss}}(t) = h(\pi(\xi(t)))$.

[6] Similar considerations can be drawn for multiple-input multiple-output (MIMO) systems, by following the framework presented in [10, 28].

[7] From now on, the dependence on t is dropped when clear from the context.

[8] Let $A \in \mathbb{R}^{n\times n}$. An eigenvalue $a \in \lambda(A)$ is said to be *simple* if its algebraic multiplicity is equal to 1.

[9] All statements are local, although global versions can be straightforwardly derived.

2.2 Model reduction by moment-matching

The reduction technique based on the notion of moments, recalled in Section 2.1, consists of the interpolation of the steady-state response of the output of the system to be reduced[10]: a reduced order model by moment-matching is such that its steady-state response *exactly matches* the steady-state response of system (1).

Following the moment-based theory of Section 2.1, the notion of a reduced order model by moment-matching for nonlinear systems can now be introduced.

Definition 2 [36] Consider the signal generator in (2). The system described by the equations

$$\begin{aligned} \dot{\Theta} &= \phi(\Theta, u), \\ \theta &= \kappa(\Theta), \end{aligned} \tag{5}$$

with $\Theta(t) \in \mathbb{R}^\nu$ and $\theta(t) \in \mathbb{R}$, is a model of system (1) at (S, L), if system (5) has the same moments at (S, L) as system (1). In addition, system (5) is a reduced order model of system (1) at (S, L) if $\nu < n$.

Lemma 2 [36] *Consider system* (1) *and the signal generator* (2)*. Suppose Assumptions 1 and 2 hold, and that the zero equilibrium of system* (1) *is locally exponentially stable. Then, system* (5) *matches the moments of system* (1) *at* (S, L) *if the partial differential equation*

$$\frac{\partial p}{\partial \xi} S\xi = \phi(p(\xi), L\xi), \tag{6}$$

has a unique solution p *such that*

$$h(\pi(\xi)) = \kappa(p(\xi)), \tag{7}$$

where the mapping π *is the unique solution of equation* (4)*.*

Following the result of Lemma 2, a family of systems achieving moment-matching at (S, L) [36] can be defined as

$$\begin{aligned} \dot{\Theta} &= (S - \rho(\Theta)L)\Theta + \rho(\Theta)u, \\ \theta &= h(\pi(\Theta)), \end{aligned} \tag{8}$$

with $\rho : \mathbb{R}^\nu \to \mathbb{R}^\nu$ a free mapping. A particularly interesting simplification can be achieved with the selection $\rho(\Theta) = \Delta$, for any constant matrix Δ. This choice produces a family of reduced order models described by a linear differential equation with a nonlinear output map, *i.e.* by a Wiener model.

Remark 6 Two advantages of the selection of the mapping $\rho(\Theta) = \Delta$, in the family of models (8), can be clearly identified: the matrix Δ can be selected to enforce additional properties on (8) such as a set of prescribed eigenvalues, and the determination of the reduced order model achieving moment-matching at (S, L) boils down to the computation of the mapping $h \circ \pi$.

Remark 7 Note that, though (8) provides a potentially powerful result, it is virtually impossible to compute an analytic expression for the moment $h \circ \pi$ for a general nonlinear mapping f, due to the nature of the nonlinear partial differential equation (4). In other words, without a proper approximation framework, the theory recalled in both Sections 2.1 and 2.2 has little practical value. This is specifically addressed in Section 5 of this paper, where we propose a suitable approximation technique, tailored for the wave energy application.

3 WEC dynamics and modelling

This section begins by recalling well-known facts behind control-oriented WEC modelling (see, for instance, [13]). For simplicity, a 1-degree-of-freedom (DoF) device is assumed, given that a similar analysis can be carried out for multi-DoF devices, by simply following the moment-based multiple-input, multiple-output approach presented in [10,11]. The equation of motion for such a WEC can be expressed in the time-domain, in terms of the following system Σ:

$$\Sigma : \begin{cases} \ddot{z} = \mathcal{M}\left(f_\mathrm{r} + f_\mathrm{re}^\mathrm{l} + f_\mathrm{e} + f_\mathrm{nl}\right), \\ y = \dot{z}, \end{cases} \tag{9}$$

where $z : \mathbb{R}^+ \to \mathbb{R}$ is the device excursion (displacement), $f_\mathrm{e} : \mathbb{R}^+ \to \mathbb{R}$, the wave excitation force (external uncontrollable input due to the incoming wave field), f_re^l the linear component of the hydrostatic restoring force, f_r the radiation force, and $\mathcal{M} \in \mathbb{R}_{>0}$ is the inverse of the generalised mass matrix of the device (see [13]). The mapping $f_\mathrm{nl} : \mathbb{R}^+ \to \mathbb{R}$, $t \mapsto f_\mathrm{nl}(t)$ represents potential nonlinear effects such as, for instance, viscous drag forces and nonlinear hydrostatic effects[11].

The linear component of the hydrostatic force can be written as $f_\mathrm{re}^\mathrm{l}(t) = -s_\mathrm{h} z(t)$, where s_h denotes the hydrostatic stiffness, which depends upon the device geometry. The radiation force f_r is modelled based on

[10] Throughout this manuscript, if a given system Σ is reduced by moment-matching to a system $\tilde{\Sigma}$, Σ and $\tilde{\Sigma}$ are referred to as the *target* and *approximating* systems, respectively.

[11] In the case of nonlinear restoring effects, the division between linear and nonlinear contributions is performed without any loss of generality, and to subsequently analyse the local properties of system (9) in Section 4.

linear potential theory and, using the well-known Cummins' equation [7], can be written as

$$f_{\mathrm{r}}(t) = -m_\infty \ddot{z}(t) - \int_{\mathbb{R}^+} k_{\mathrm{r}}(\tau)\dot{z}(t-\tau)d\tau, \tag{10}$$

where $m_\infty = \lim_{\omega\to+\infty} A(\omega) > 0$ is the added-mass at infinite frequency, $A(\omega)$ is the radiation added mass[12] and $k_{\mathrm{r}} : \mathbb{R}^+ \to \mathbb{R}^+$, $k_r \in L^2(\mathbb{R})$, is the (causal) radiation impulse response function containing the memory effect of the fluid response. Finally, the equation of motion of the WEC is given by

$$\Sigma : \begin{cases} \ddot{z} = \mathcal{M}\left(-k_{\mathrm{r}} * \dot{z} - s_{\mathrm{h}} z + f_{\mathrm{e}} + f_{\mathrm{nl}}\right), \\ y = \dot{z}. \end{cases} \tag{11}$$

Note that (non-parametric) equation (11) is of a Volterra integro-differential form, specifically of the convolution class[13].

4 Nonlinear moment-based WEC formulation for model reduction

The nonlinear moment-based theory, recalled and discussed in Section 2, directly depends on the availability of a state-space representation of the system to be reduced, which is not the case for the non-parametric equation described by system Σ in (11). In the light of this, the following equivalent representation is proposed:

$$\Sigma : \begin{cases} \dot{w} = f(w, f_{\mathrm{e}}) = Aw + B(f_{\mathrm{e}} - k_{\mathrm{r}} * Cw) + \hat{f}(w), \\ y = h(w) = Cw, \end{cases} \tag{12}$$

for $t \in \mathbb{R}^+$, where $w(t) = \left[z(t)\ \dot{z}(t)\right]^\intercal \in \mathbb{R}^2$ contains the displacement and velocity corresponding to system Σ, and the (constant) matrices $A \in \mathbb{R}^{2\times 2}$, $B \in \mathbb{R}^2$ and $C^\intercal \in \mathbb{R}^2$ are defined as

$$A = \begin{bmatrix} 0 & 1 \\ -\mathcal{M}s_{\mathrm{h}} & 0 \end{bmatrix}, \quad B = \begin{bmatrix} 0 \\ \mathcal{M} \end{bmatrix}, \quad C = \begin{bmatrix} 0 \\ 1 \end{bmatrix}^\intercal. \tag{13}$$

The nonlinear mapping $\hat{f} : \mathbb{R}^2 \to \mathbb{R}^2$ is given by

$$\hat{f}(w) = \begin{bmatrix} 0 \\ \mathcal{M}f_{\mathrm{nl}}(w) \end{bmatrix} = Bf_{\mathrm{nl}}(w). \tag{14}$$

Remark 8 In line with the most utilised nonlinear effects in WEC control/estimation applications (see [8]), it is assumed that the mapping f_{nl} depends only on w, *i.e.* the displacement and velocity of the WEC system involved. Nevertheless note that, if required by a particular application, a more general class of nonlinear effects can be straightforwardly considered, such as, for instance, non-ideal PTO dynamics [3].

Within the moment-based theory recalled in Section 2, the mapping corresponding to the external input f_{e} is written in terms of an autonomous single-output signal generator (analogously to the case of equation (2)), *i.e.* the set of equations

$$\begin{aligned} \dot{\xi} &= S\xi, \\ f_{\mathrm{e}} &= L\xi, \end{aligned} \tag{15}$$

for $t \in \mathbb{R}^+$, with $\xi(t) \in \mathbb{R}^\nu$, $S \in \mathbb{R}^{\nu\times\nu}$ and $L^\intercal \in \mathbb{R}^\nu$. The set of standing assumptions, *i.e.* Assumptions 1 and 2, are ensured as follows.

Assumption 2, which concerns the definition of the spectrum of the matrix S, is addressed by recalling (see, for instance, [24]) that ocean waves are numerically generated as a finite sum of harmonics of a so-called *fundamental frequency* ω_0. To be precise, let $\mathscr{F} = \{h_p\omega_0\}_{p=1}^{\mathbf{f}} \subset \mathbb{R}^+$, where $\mathcal{H} = \{h_p\}_{p=1}^{\mathbf{f}} \subset \mathbb{N}_{\geq 1}$, with $h_1 < \ldots < h_{\mathbf{f}}$, be a set composed of a finite number of harmonics of the fundamental frequency ω_0. In particular, the matrix S is defined in a block-diagonal form as

$$S = \bigoplus_{p=1}^{\mathbf{f}} \begin{bmatrix} 0 & h_p\omega_0 \\ -h_p\omega_0 & 0 \end{bmatrix}, \tag{16}$$

where $\nu = 2\mathbf{f}$, $\mathbf{f} \in \mathbb{N}_{\geq 1}$, and the spectrum of S is given by $\lambda(S) = (j\mathscr{F}) \cup (-j\mathscr{F}) \subset \mathbb{C}^0$, so that Assumption 2 clearly holds.

With respect to Assumption 1, this condition is ensured (without any loss of generality) as follows: From now, the output vector L is given by a Hadamard identity on the space $\mathbb{R}^{1\times\nu}$, *i.e.* $L^\intercal = \mathbf{1}_\nu$, so that the minimality of the triple $(\mathbf{1}_\nu^\intercal, S, \xi(0))$ holds as long as the pair $(S, \xi(0))$ is excitable. The specific choice for the structure of $\xi(0)$ is discussed in the following remark.

Remark 9 (On the definition of $\xi(0)$) Let $\xi(0) = \sum_{p=1}^{\mathbf{f}} e_p^{\mathbf{f}} \otimes \left[\alpha_p\ \beta_p\right]^\intercal$, where the set of coefficients $\{\alpha_p, \beta_p\}_{p=1}^{\mathbf{f}} \subset \mathbb{R}$. Then, the vector ξ can be expanded as

$$\xi(t) = e^{St}\xi(0) = \sum_{p=1}^{\mathbf{f}} e_p^{\mathbf{f}} \otimes \begin{bmatrix} {}^p\xi^+(t) \\ {}^p\xi^-(t) \end{bmatrix}, \tag{17}$$

where the mappings ${}^p\xi$ are defined as

$$\begin{aligned} {}^p\xi^+ &: \mathbb{R}^+ \to \mathbb{R}, \quad t \mapsto \alpha_p \cos(h_p\omega_0 t) + \beta_p \sin(h_p\omega_0 t), \\ {}^p\xi^- &: \mathbb{R}^+ \to \mathbb{R}, \quad t \mapsto \beta_p \cos(h_p\omega_0 t) - \alpha_p \sin(h_p\omega_0 t). \end{aligned} \tag{18}$$

[12] See [13] for the definition of $A(\omega)$.

[13] The interested reader is referred to [42] for further detail on this class of integro-differential operators.

Remark 10 Note that the excitability condition on the pair $(S, \xi(0))$ holds as long as α_p and β_p are not simultaneously zero, for all $p \in \mathbb{N}_{\mathbf{f}}$.

Remark 11 Let the sets of functions $\mathscr{X}_\xi^{\mathbf{f}} = \{{}^p\xi^+, {}^p\xi^-\}_{p=1}^{\mathbf{f}}$ and $\mathscr{X}_0^{\mathbf{f}} = \{\cos(h_p\omega_0 t), \sin(h_p\omega_0 t)\}_{p=1}^{\mathbf{f}}$. Note that, given the excitability condition on the pair $(S, \xi(0))$, it is straightforward to check that $\text{span}\{\mathscr{X}_\xi^{\mathbf{f}}\} = \text{span}\{\mathscr{X}_0^{\mathbf{f}}\}$. As a consequence, the input f_e is always T-periodic, where $T = 2\pi/\omega_0 \in \mathbb{R}^+$ is the *fundamental period*[14] of f_e.

The following standard assumption on the nonlinear mapping $\hat{f}$ is posed to later prove existence and uniqueness of the nonlinear moment of system (12) at the signal generator (S, L).

Assumption 3 *The mapping $\hat{f} : \mathbb{R}^2 \to \mathbb{R}^2$ is such that*

$$\hat{f}(0) = 0, \qquad \left.\frac{\partial \hat{f}(w)}{\partial w}\right|_{w=0} = 0. \tag{19}$$

Note that this assumption is without loss of generality, since the matrices in (12), and the mapping $\hat{f}$, can always be redefined to satisfy it[15].

Finally, an assumption on the stability in the first approximation of system (12), is introduced.

Assumption 4 *The zero equilibrium of system*

$$\dot{w} = Aw - B(k_\text{r} * Cw), \tag{20}$$

is asymptotically stable in a Lyapunov sense.

As discussed in several studies, such as [13,37], the linear equation of motion (20) is asymptotically stable for any meaningful values of the involved parameters (and impulse response function k_r). Thus, this assumption is, in practice, also without loss of generality.

Lemma 3 *Consider the WEC system* (12) *and the signal generator* (15)-(16)*. Suppose the triple $(L, S, \xi(0))$ is minimal, and Assumption 3 and 4 hold. Then, there exists a unique mapping π, locally defined in a neighborhood Ξ of $\xi = 0$, which solves the partial differential equation*

$$\frac{\partial \pi(\xi)}{\partial \xi} S\xi = f(\pi(\xi), L\xi), \tag{21}$$

and the moment of system (12) *at the signal generator (S, L), i.e. the mapping $h \circ \pi$, computed along a particular trajectory $\xi(t)$, coincides with the well-defined steady-state output response of such an interconnected system, i.e. $y_{ss}(t) = h(\pi(\xi(t)))$.*

Proof Let $L^\intercal = \mathbf{1}_\nu$ and let the initial condition $\xi(0)$ be as defined in Remark 10. Then, it is straightforward to check that minimality of the triple $(L, S, \xi(0))$ holds. Moreover, note that the signal generator defined in equations (15)-(16) is always such that $\lambda(S) \subset \mathbb{C}^0$ with simple eigenvalues, in line with Assumption 2. Therefore, Lemma 3 automatically holds as long as the zero equilibrium of system $\dot{w} = f(w, 0)$ is locally exponentially stable (see Lemma 1). Since this is ensured by Assumption 4, the claim follows.

In slightly different words, Lemma 3 guarantees that the steady-state response of system (12), driven by (15), can be effectively computed using the corresponding (well-defined) moment at (S, L). In particular, and following the result of Lemma 2, a family of reduced models achieving moment-matching at (S, L) of order (dimension) $\nu = 2\mathbf{f}$, for the WEC system defined in equation (11) (alternatively (12)), can be written in terms of the mapping $h \circ \pi$, with π the solution of (21), as

$$\begin{aligned} \dot{\Theta} &= (S - \Delta L)\Theta + \Delta f_\text{e}, \\ \tilde{y} &= h(\pi(\Theta)) = C\pi(\Theta), \end{aligned} \tag{22}$$

with $\Delta \in \mathbb{R}^\nu$ a free (design) parameter.

Remark 12 If the mapping π is effectively known, the family of models (22) *exactly* matches the steady-state response of the target nonlinear WEC system Σ at the signal generator (S, L).

Remark 13 The family of models defined in (22) is input-to-state *linear*, and any nonlinear effects are (statically) present in the output mapping $h \circ \pi$ (*i.e.* (22) is described by a Wiener model). Note that the set $\lambda(S - \Delta L)$ can be assigned arbitrarily, as a consequence of the observability of the pair (S, L).

Remark 14 Unlike the nonlinear system Σ in (11), which is effectively non-parametric, the family of systems achieving moment-matching at (S, L) is in state-space form. In other words, this model reduction process not only reduces complexity, but inherently computes a parametric form for the WEC system, in a single 'step'.

Though the family of models in (22) provides a strong set of candidates to tackle the nonlinear model reduction problem for WECs, there is clearly an intrinsic downside to its definition: As discussed in Section 2, even if the existence and uniqueness of π (the solution

[14] Practical implications of both $\mathbf{f}$ and T (or, equivalently, ω_0) in our model reduction framework, are discussed in detail in Section 8.1.

[15] This claim, which directly relates to Jacobian analysis, is considered standard in nonlinear dynamics. Further detail can be found in, for instance, [20, Chapter 8].

of (21)) are guaranteed by the result of Lemma 3, it is virtually impossible to compute its analytic expression, given the nonlinearity of the mapping f. In other words, the family of models defined in (22) lacks any practical value, unless one can appropriately approximate the mapping π. This is explicitly addressed in the following section.

5 On the approximation of π

The very nature of the mapping π intrinsically depends on both the characteristics of the signal generator (15), and the system dynamics (12) defined by the mapping f. The following lemma, which is analogous to [12, Proposition 2], is introduced, aiming to formally characterise π.

Lemma 4 *Suppose the triple $(L, S, \xi(0))$ is minimal, and that Assumptions 3 and 4 hold. Then, for a given trajectory $\xi(t)$, each element of the mapping π, which solves equation (21), i.e. π_i, with $i \in \mathbb{N}_2$, belongs to the Hilbert space $L^2(\mathcal{T})$ with $\mathcal{T} = [0, T] \subset \mathbb{R}^+$, where $T = 2\pi/\omega_0$.*

Proof Given the nature of the signal generator defined in equation (15), the function f_e is T-periodic, with $T = 2\pi/\omega_0$ (see Remark 11). Moreover, under the above assumptions, the zero equilibrium of $\dot{w} = f(w, 0)$ is locally exponentially stable and its (well-defined) steady-state solution is also T-periodic [21, Section VI], *i.e.* $w_{ss}(t) = w_{ss}(t - T)$. Given that, under the minimality of the triple $(L, S, \xi(0))$ and Assumptions 3 and 4, $w_{ss}(t) = \pi(\xi(t))$ (see Lemma 3), it is straightforward to conclude that each element of the mapping π belongs to $L^2(\mathcal{T})$.

Following the characterisation offered in the result of Lemma 4, and aiming to propose a method to approximate π, let the family of complex-valued mappings $\Omega_q^{\mathbb{C}} : \mathbb{R}^\nu \to \mathbb{C}$, $\xi \mapsto \Omega_q^{\mathbb{C}}(\xi)$, with $q \in \mathbb{N}_{\geq 1}$, be defined such as

$$\Omega_q^{\mathbb{C}}(\xi) = \sum_{p=1}^{\mathbf{f}} (\gamma_p \xi)^{q/h_p}, \tag{23}$$

where $\gamma_p^\intercal \in \mathbb{C}^\nu$ is such that $\gamma_p^\intercal = e_{2p-1}^\nu + j e_{2p}^\nu$, for all $p \in \mathbb{N}_{\mathbf{f}}$. This mapping can be effectively used to span $L^2(\mathcal{T})$, as explicitly demonstrated in the following lemma.

Lemma 5 *Let $\mathscr{X}_0^k = \{\cos(q\omega_0 t), \sin(q\omega_0 t)\}_{q=1}^k$ be a canonical set in $L^2(\mathcal{T})$, with $\mathcal{T} = [0\ T] \subset \mathbb{R}^+$, $T = 2\pi/\omega_0$, and consider the family of real-valued functions*

$$\begin{aligned} &\Omega_q^+ : \mathbb{R}^\nu \to \mathbb{R}, \quad \xi \mapsto \Re\left\{\Omega_q^{\mathbb{C}}(\xi)\right\}, \\ &\Omega_q^- : \mathbb{R}^\nu \to \mathbb{R}, \quad \xi \mapsto \Im\left\{\Omega_q^{\mathbb{C}}(\xi)\right\}. \end{aligned} \tag{24}$$

Let the set $\mathscr{X}_\Omega^k = \{\Omega_q^+(\xi), \Omega_q^-(\xi)\}_{q=1}^k$. Then,

$$\text{span}\{\mathscr{X}_\Omega^k\} = \text{span}\{\mathscr{X}_0^k\}. \tag{25}$$

Proof Note that the key term, composing the family of complex-valued mappings in (23), can be alternatively written as

$$\gamma_p \xi = {}^p\xi^+ + j\,{}^p\xi^- \in \mathbb{C}, \tag{26}$$

for all $p \in \mathbb{N}_{\mathbf{f}}$, and where each of the mappings ${}^p\xi^+$ and ${}^p\xi^-$ are defined as in equation (18) (see also Remark 9). Moreover, note that these functions can be equivalently written as,

$$\begin{aligned} {}^p\xi^+(t) &= \Re\left\{(\alpha_p + j\beta_p)e^{jh_p\omega_0 t}\right\}, \\ {}^p\xi^-(t) &= \Im\left\{(\alpha_p + j\beta_p)e^{jh_p\omega_0 t}\right\}, \end{aligned} \tag{27}$$

so that, clearly, the following expression

$$(\gamma_p\xi)^{q/h_p} = \left({}^p\xi^+ + j\,{}^p\xi^-\right)^{q/h_p} = (\alpha_p + j\beta_p)^{q/h_p} e^{jq\omega_0 t}, \tag{28}$$

for all $p \in \mathbb{N}_{\mathbf{f}}$ and $q \in \mathbb{N}_{\geq 1}$, holds. In other words, only the q-th harmonic of the fundamental frequency, *i.e.* $q\omega_0$, is present in the output of the complex-valued mapping $\Omega_q^{\mathbb{C}}$. Given the excitability condition on the pair $(S, \xi(0))$, α_p and β_p cannot be simultaneously zero, for all $p \in \mathbb{N}_{\mathbf{f}}$ (see Remark 10), so that $\text{span}\{\Omega_q^+(\xi), \Omega_q^-(\xi)\} = \text{span}\{\cos(q\omega_0 t), \sin(q\omega_0 t)\}$, and the proof follows.

Remark 15 Naturally, the set $\mathscr{X}_\Omega^k$ forms an orthogonal basis of $L^2(\mathcal{T})$, under the standard inner-product operator of such a space, as $k \to \infty$.

The result of Lemma 5, together with Remark 15, allows each element of the mapping π, *i.e.* π_i, with $i \in \mathbb{N}_2$, to be uniquely expressed in terms of the set $\mathscr{X}_\Omega^k$ as a linear combination of its elements (see, for instance, [2]), *i.e.*

$$\pi_i(\xi) = \sum_{q=1}^{k} \begin{bmatrix} c_q^+ & c_q^- \end{bmatrix} \begin{bmatrix} \Omega_q^+(\xi) \\ \Omega_q^-(\xi) \end{bmatrix} + \epsilon_i(\xi) = \tilde{\Pi}_i \Omega^k(\xi) + \epsilon_i(\xi), \tag{29}$$

with $\Omega^k(\xi(t)) \in \mathbb{R}^{2k}$ such that $\Omega^k(\xi) = \sum_{q=1}^k e_q^k \otimes \left[\Omega_q^+(\xi)\ \Omega_q^-(\xi)\right]^\intercal$, and where the mapping $\epsilon_i : \mathbb{R}^\nu \to \mathbb{R}$ is given by,

$$\epsilon_i(\xi) = \sum_{q=k+1}^{+\infty} \begin{bmatrix} c_q^+ & c_q^- \end{bmatrix} \begin{bmatrix} \Omega_q^+(\xi) \\ \Omega_q^-(\xi) \end{bmatrix}. \tag{30}$$

Remark 16 Note that, following equation (29), π can be compactly expressed as

$$\pi(\xi) = \begin{bmatrix}\tilde{\Pi}_1\\ \tilde{\Pi}_2\end{bmatrix} \Omega^k(\xi) + \begin{bmatrix}\epsilon_1(\xi)\\ \epsilon_2(\xi)\end{bmatrix} = \tilde{\Pi}\Omega^k(\xi) + E(\xi), \quad (31)$$

where the operator $E : \mathbb{R}^\nu \to \mathbb{R}^2$ is the *truncation* error.

If the truncation error E is 'ignored', the mapping π can be effectively approximated as $\pi \approx \tilde{\pi}(\xi) = \tilde{\Pi}\Omega^k(\xi)$, *i.e.* by its expansion on the $2k$-dimensional set $\mathscr{X}_\Omega^k$. This motivates the following key definition.

Definition 3 The mapping $h \circ \tilde{\pi}$, where $\tilde{\pi}(\xi) = \tilde{\Pi}\Omega^k(\xi)$, is the *approximated* moment of system (12) at the signal generator (S, L).

With this definition, and following equation (22), a family of reduced models of order (dimension) $\nu = 2\mathbf{f}$, for the WEC system defined in equation (11), can be written in terms of the approximated moment (see Definition 3) as

$$\Sigma \approx \tilde{\Sigma} : \begin{cases}\dot{\Theta} = (S - \Delta L)\Theta + \Delta f_{\mathrm{e}},\\ \tilde{y} = C\tilde{\Pi}\Omega^k(\Theta),\end{cases} \quad (32)$$

parameterised by the design matrix $\Delta \in \mathbb{R}^\nu$.

Remark 17 Note that not only is the family of systems (32) input-to-state linear, but the user also has full control over the complexity of the output mapping, *i.e.* one can define how 'complex' Ω^k is by simply adjusting the number k of harmonics utilised to approximate π with $\tilde{\pi}$. We note that a natural trade-off arises when selecting k: While a higher value for k implies a better approximating mapping $\tilde{\pi}$ (see also Remark 19), it also intrinsically increases the complexity of the output mapping in (32).

Within the proposed framework, the computation of a reduced system by moment-matching, as defined in equation (32), now boils down to the computation of the matrix $\tilde{\Pi}$, for a given selection of order k in Ω^k, *i.e.* a given number of harmonic functions associated with the fundamental frequency ω_0 (dictated by the nature of the input f_{e}). This is specifically addressed in Section 5.1.

5.1 A Galerkin-like approach

Aiming to propose a method to compute $\tilde{\Pi}$, and inspired by the family of mean weighted residual methods [4,14], the following *residual* mapping $r : \mathbb{R}^2 \to \mathbb{R}^2$ can be defined as

$$r(\tilde{\Pi}\Omega^k(\xi)) := \tilde{\Pi}\frac{\partial\Omega^k(\xi)}{\partial\xi}S\xi - f(\tilde{\Pi}\Omega^k(\xi), L\xi), \quad (33)$$

which directly arises from 'replacing' the mapping π by the approximating function $\tilde{\pi}$ in equation (21).

Following the so-called Galerkin (or spectral) approach (see, for instance, [41]), which effectively belongs to the so-called family of mean weighted residual methods [14], the constant matrix $\tilde{\Pi}$ can be computed by projecting the residual mapping onto the space spanned by the set of k harmonics of the fundamental frequency defined by $\mathscr{X}_\Omega^k$, *i.e.* the entries of $\Omega_\Omega^k(\xi)$. In contrast to the 'traditional' Galerkin formulation, a *Galerkin-like* method is proposed, as detailed in the following.

Let $\Omega_0^k(t) = \sum_{q=1}^k e_q^k \otimes \left[\cos(q\omega_0 t) - \sin(q\omega_0 t)\right]^\intercal \in \mathbb{R}^{2k}$ be a vector containing the $2k$ canonical harmonic functions on $L^2(\mathcal{T})$. Then, given a fixed trajectory $\xi(t)$, the constant matrix $\tilde{\Pi} \in \mathbb{R}^{2\times 2k}$ can be computed by zeroing the projection of the residual mapping onto the set spanned by the elements (entries) of the vector Ω_0^k, *i.e.* as the solution of the following algebraic system of $4k$ equations:

$$\left\langle r(\tilde{\Pi}\Omega^k(\xi)), \Omega_0^{k\intercal} \right\rangle = 0, \quad (34)$$

where $\langle\ \rangle$ denotes the inner-product operator in $L^2(\mathcal{T})$, as defined in Section 1.1.

Remark 18 In the proposed Galerkin-like approach, the canonical vector Ω_0^k is utilised when projecting the residual mapping, instead of the entries of Ω^k (which would be the case in a 'traditional' Galerkin method [4]). This substantially simplifies the computation of the projections involved in (34), which are effectively inner-product operations in $L^2(\mathcal{T})$. This simplification is specifically discussed in Section 6.1.

Remark 19 The existence of solutions of equation (34), under the hypothesis of Lemma 4, is always guaranteed for all sufficiently large k [41]. Moreover, the approximated moment $\tilde{\pi}(\xi) = \tilde{\Pi}\Omega^k(\xi)$ converges uniformly towards the exact solution (31) as $k \to \infty$ (see also [41]).

Remark 20 The system of algebraic equations (34) on the $4k$ entries of $\tilde{\Pi}$, can be computed using state-of-the-art root finding algorithms, such as those described in, for instance, [6].

6 Practical aspects and considerations

6.1 Projection of the residual mapping

This section begins by noting that the selection of the vector Ω_0^k, involved in the projection of the residual mapping within the Galerkin-like approach proposed in Section 5.1, has a very specific purpose, which is

detailed in the following. Recall that the Fourier transform of a T-periodic function, *i.e.* a function $x \in L^2(\mathcal{T})$, is always well-defined, and can be computed with the expression

$$\begin{aligned} X(\omega) &= \int_{\mathcal{T}} x(t) e^{-j\omega t} dt \\ &= \int_{\mathcal{T}} x(t)\cos(\omega t) dt - i \int_{\mathcal{T}} x(t)\sin(\omega t) dt. \end{aligned} \tag{35}$$

Note that, due to the specific selection of the entries of Ω_0^k, each of the inner-product operations involved in the Galerkin-like method proposed in (34) are, effectively, either the real or the imaginary parts of the Fourier transform of the residual mapping r, evaluated at each of the k harmonics of the fundamental frequency ω_0, *i.e.* at the set $\{q\omega_0\}_{q=1}^k$. In other words, the system of equations (34) characterising $\tilde{\Pi}$ can be equivalently written as

$$\left[\Re\{R(\omega_0)\}\ \Im\{R(\omega_0)\}\ \dots\ \Re\{R(k\omega_0)\}\ \Im\{R(k\omega_0)\}\right] = 0, \tag{36}$$

where $R : \mathbb{R} \to \mathbb{C}^2$ denotes the Fourier transform of the residual mapping r.

Remark 21 The evaluation of the Fourier transform at each frequency $q\omega_0$, can be done both efficiently and robustly using well-established fast Fourier transform (FFT) algorithms (see, for instance, [32]).

6.2 Extension to multiple trajectories

Until this point, a single trajectory $\xi(t)$ has been considered, *i.e.* a single initial condition $\xi(0)$ for the signal generator (S, L). In other words, a single input $f_e(t) = Le^{St}\xi(0)$ has been taken into account for the computation of the approximating $\tilde{\pi}$. Though this might be appropriate for some cases, such as, for instance, the case of WECs under (deterministic) regular wave excitation (further discussed in Section 7.1), constraining the approximation method to a single initial condition can be limiting for the case of WEC systems subject to irregular wave excitation. This issue is addressed, for the Galerkin-like approach of Section 5.1, as follows[16].

Let $\xi(0) \in \Xi$, where $\Xi = \{\zeta_i\}_{i=1}^l \subset \mathbb{R}^\nu$ represents a set with l initial conditions[17], defined in a neighbourhood of $\xi = 0$. Suppose the pairs of matrices (S, ζ_i) are excitable for all $i \in \mathbb{N}_l$. Let the vector ξ, generated as a function of the initial condition ζ_i, be denoted as $\xi_{\zeta_i} = e^{St}\zeta_i$. Then, the Galerkin-like procedure, proposed in Section 5.1, can be adapted for the case of multiple trajectories, where the constant matrix $\tilde{\Pi}$, which completely characterises the approximating mapping $\tilde{\pi}(\xi) = \tilde{\Pi}\Omega^k(\xi)$, is computed in terms of a minimisation procedure:

$$\min_{\tilde{\Pi}\in\mathbb{R}^{2\times 2k}} \left\| \begin{bmatrix} \left\langle r(\tilde{\Pi}\Omega^k(\xi_{\zeta_1})), \Omega_0^k(\xi_{\zeta_1}) \right\rangle \\ \vdots \\ \left\langle r(\tilde{\Pi}\Omega^k(\xi_{\zeta_l})), \Omega_0^k(\xi_{\zeta_l}) \right\rangle \end{bmatrix} \right\|_{\mathrm{F}}^2, \tag{37}$$

where the inner product operations, for each initial condition ζ_i, with $i \in \mathbb{N}_l$, can be computed using FFT operations, as detailed in Section 6.1.

The minimisation procedure described in equation (37) is effectively utilised both for the case of nonlinear model reduction by moment-matching for WECs under regular, and irregular, wave excitation, further discussed and illustrated in Sections 7 and 8, respectively.

6.3 Modifications to the mapping Ω^k

This section introduces a modification for the vector valued function Ω^k, utilised to approximate the nonlinear moment of system (11) at the signal generator (15), aiming to 'simplify' the description of the output mapping involved in (22). In particular, one can modify the entries of $\Omega^k(\xi)$ such that only integer exponents of ξ are required, and a fixed maximum number of harmonics associated with a given multiple $h_p\omega_0$, involved in the definition of the matrix S in equation (16), is considered, for each $p \in \mathbb{N}_f$. This is explicitly addressed in the following.

Let $k_p^{\max}$ denote the maximum number of harmonics of a given multiple of the fundamental frequency $h_p\omega_0$, with $p \in \mathbb{N}_{\mathbf{f}}$. Then, the complex-valued mapping $\Omega_q^{\mathbb{C}}$ defined in equation (23), which fully characterises the entries of Ω^k, can be modified as follows:

$$\Omega_q^{\mathbb{C}}(\xi) = \sum_{p=1}^{\mathbf{f}} a_{qp}(\gamma_p\xi)^{q/h_p}, \tag{38}$$

where the coefficients a_{qp} are defined as

$$a_{qp} = \begin{cases} 1 & \text{if } \mathrm{mod}(q, h_p) = 0 \quad \wedge \quad \frac{q}{h_p} \le k_p^{\max}, \\ 0 & \text{if } \mathrm{mod}(q, h_p) \neq 0 \quad \vee \quad \frac{q}{h_p} > k_p^{\max}, \end{cases} \tag{39}$$

and $\mathrm{mod} : \mathbb{N} \times \mathbb{N}_{\geq 1} \to \mathbb{N}$ denotes the modulo operator.

[16] The extension to multiple trajectories presented in this section is proposed in the spirit of the so-called $\mathscr{U}/\mathscr{X}$ variation [35].

[17] The selection of l depends upon the specific nature of the WEC input process. This is discussed in detailed in Sections 7 and 8.

Remark 22 With the introduction of this set of coefficients a_{qp}, the mapping Ω^k *only depends* on natural powers involving the entries of ξ, *i.e.* it becomes *polynomial*. In other words, the output of the reduced model $\tilde{y}$ (32) is always smooth. Note that this modification does not pose any loss of generality with respect to (23) as long as $\omega_0 \in \mathscr{F}$.

To clarify the use and 'evolution' of the set of coefficients a_{qp}, for a given signal generator, an illustrative example is considered in the following. Let the fundamental frequency be $\omega_0 = 1$ and consider a signal generator with a dynamic matrix S given by

$$S = \begin{bmatrix} 0\,1 & 0\,0 & 0\,0 \\ -1\,0 & 0\,0 & 0\,0 \\ 0\,0 & 0\,3 & 0\,0 \\ 0\,0 & -3\,0 & 0\,0 \\ 0\,0 & 0\,0 & 0\,4 \\ 0\,0 & 0\,0 & -4\,0 \end{bmatrix}, \tag{40}$$

where, clearly, the set of coefficients $\mathcal{H} = \{h_p\}_{p=1}^3$ is given by $h_1 = 1$, $h_2 = 3$ and $h_3 = 4$. Suppose the maximum number of harmonics associated with each h_p, to compute the vector Ω^k, are set to $k_1^{\max} = 10$, $k_2^{\max} = 3$ and $k_3^{\max} = 2$. The coefficients a_{qp} are illustrated, for this example case, in Figure 1, with $q \in \mathbb{N}_{10}$. Non-zero values of a_{qp} are indicated with a black dot.

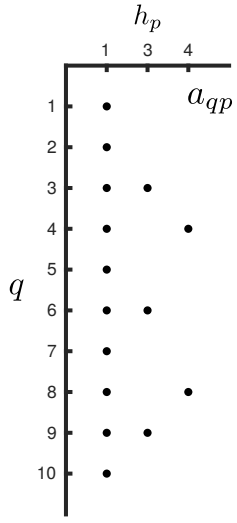

Fig. 1 Coefficients a_{qp} for the mapping Ω^k, for $h_1 = 1$, $h_2 = 3$ and $h_3 = 4$, where $q \in \mathbb{N}_{10}$. Non-zero values of a_{qp} are indicated with a black dot.

6.4 On the eigenvalues of the reduced model

As discussed in Remark 13, the family of reduced models by moment-matching defined in equation (32) is input-to-state linear. Furthermore, the eigenvalues characterising such a system, *i.e.* the set $\lambda(S - \Delta L)$, can be assigned arbitrarily, as a consequence of the observability of the pair (S, L).

It is proposed to assign such a set of eigenvalues using information from the Jacobian linearisation of system (11) about the origin, *i.e.* the non-parametric *linear* Cummins' equation (20). In particular, one can estimate a set $\Lambda \subset \mathbb{C}_{<0}$ of ν eigenvalues for system (20) in terms of the singular value decomposition of the Hankel matrix $\hat{H}$, constructed from the input-output frequency-domain data of the WEC (see [10] for further detail).

Once this set Λ is obtained, the matrix Δ can always be computed such that $\lambda(S - \Delta L) = \Lambda$, due to the observability of (S, L), using standard algorithms (such as, for instance, [22]).

7 WEC systems under regular wave excitation

To illustrate the performance of the model reduction by moment-matching technique presented in this paper, a clear distinction has to be made, in terms of the nature of the wave excitation input, *i.e.* regular or irregular. In particular, this section analyses a WEC system under regular wave excitation, assuming two different cases concerning the wave height: Deterministic and stochastic.

Remark 23 Though the simplistic nature behind regular waves effectively misrepresents a realistic sea-state, this type of waves are commonly considered in the WEC literature to derive results of theoretical interest, providing valuable insight into, for instance, the underlying dynamics of a floating body. In addition, note that the analysis provided in this section motivates the methodology proposed for the more complex irregular wave input case (which effectively represents a realistic sea-state), described in Section 8.

For the remainder of this section, a spherical heaving point absorber WEC is considered, with a radius of 2.5 [m]. Such a geometry is schematically illustrated in Figure 2.

The nonlinear mapping f_{nl}, characterising the nonlinear effects present in the non-parametric WEC equation (11) (alternatively (12)), is assumed to be given, for this spherical heaving point absorber case, by:

$$\begin{aligned} f_{\text{nl}}(z, \dot{z}) &= f_{\text{re}}^{\text{nl}}(z) + f_v(\dot{z}), \\ f_{\text{re}}^{\text{nl}}(z) &= \frac{1}{3}\rho g \pi z^3, \\ f_v(\dot{z}) &= -2\rho\pi(2.5)^2 C_d \dot{z}|\dot{z}|, \end{aligned} \tag{41}$$

where ρ is the water density, g the gravitational constant, and f_v and $f_{\text{re}}^{\text{nl}}$ represent nonlinear viscous and hydrostatic restoring effects, respectively[18]. The value for the viscous drag coefficient is set to $C_d = 1$, following the study on consistency of viscous drag identification for WECs, performed in [18].

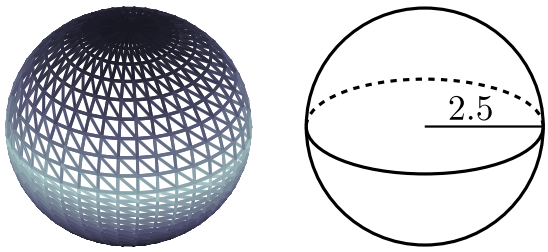

Fig. 2 Spherical heaving point absorber WEC considered for the case of nonlinear model reduction under regular wave excitation.

To illustrate the proposed nonlinear model reduction by moment-matching technique for devices under regular excitation, it is assumed that the WEC is subject to regular waves with a given frequency ω^* and height H_w. As a matter of fact, note that ω^* is indeed the fundamental frequency defined in Section 4, *i.e.* $\omega_0 = \omega^*$. Under these conditions, the wave excitation input f_{e} can be written as,

$$f_{\text{e}}(t) = A^* \cos(\omega^* t), \tag{42}$$

where $A^* = |K_{\text{e}}(\omega^*)|\frac{H_w}{2} \in \mathbb{R}^+$, with $K_{\text{e}} : \mathbb{R} \to \mathbb{C}$ the Fourier transform of the so-called excitation impulse response function (see, for instance, [13]). This input can be clearly generated following Section 4, *i.e.* as the output of a signal generator, analogously to equation (15), characterised by the one-dimensional set $\mathscr{F} = \{\omega^*\}$:

$$\begin{aligned} \dot{\xi} &= S\xi = \begin{bmatrix} 0 & \omega^* \\ -\omega^* & 0 \end{bmatrix} \xi, \\ f_e &= L\xi = \begin{bmatrix} 1 & 1 \end{bmatrix} \xi, \\ \xi(0) &= \begin{bmatrix} \alpha & \beta \end{bmatrix}^\intercal = \begin{bmatrix} \frac{A^*}{2} & \frac{A^*}{2} \end{bmatrix}^\intercal. \end{aligned} \tag{43}$$

A clear distinction is now made with respect to the nature of the wave height H_w and, hence, the amplitude A^* of the excitation signal f_{e}. In particular, if the wave height is assumed to be fixed and known, then a single initial condition $\xi(0)$ (as in equation (43)) is required to fully characterise the approximating moment and, hence, the corresponding reduced order model by moment-matching. This case is referred to as *deterministic regular excitation*, and is illustrated and discussed in Section 7.1. In contrast, if the wave height is only known to lie within a given set, then a set of multiple initial conditions is required to characterise the corresponding reduced order model, by following Section 6. This case is referred to as *stochastic regular excitation*, and is illustrated and discussed in Section 7.2.

[18] The mapping $f_{\text{re}}^{\text{nl}}$ is geometry dependent and, for the spherical heaving point absorber case, can be found in, for instance, [25].

7.1 Deterministic regular excitation

Recall that, for this regular excitation case, the so-called fundamental frequency ω_0 is indeed ω^*. As discussed previously in Section 7, if the wave height is fixed and known, then a single initial condition $\xi(0)$ is required to fully characterise the reduced order model by moment-matching, defined in equation (32). To be precise, the computation of the matrix $\tilde{\Pi}$, fully characterising the approximating moment (as in Definition 3), can be computed using the Galerkin-like approach proposed in Section 5.1, without any further modifications. This case is explicitly discussed in the following.

Let $\omega^* = 0.8$ [rad/s], which corresponds with a wave period of approximately $T_w = 8$ [s], and suppose the wave height, which characterises the amplitude A^* of the wave excitation force, is fixed at $H_w = 2$ [m]. A nonlinear model, reduced by moment-matching, for the heaving sphere considered in this section, can be computed directly from (32) as

$$\Sigma \approx \tilde{\Sigma} : \begin{cases} \dot{\Theta} = \left(\begin{bmatrix} 0 & 0.8^* \\ -0.8^* & 0 \end{bmatrix} - \Delta \begin{bmatrix} 1 & 1 \end{bmatrix} \right) \Theta + \Delta f_{\text{e}}, \\ \tilde{y} = C\tilde{\Pi}\Omega^k(\Theta), \end{cases} \tag{44}$$

where the mapping Ω^k is characterised by equation (24), for a given number of harmonics k of the fundamental frequency ω^*, and where the matrix $\tilde{\Pi}$ is computed following Section 5.1. Note that the initial condition $\xi(0)$, involved in the computation of $\tilde{\Pi}$, is exactly as described in equation (43). The matrix Δ, assigning the eigenvalues of the reduced model (44), is computed following Section 6.4.

Remark 24 Given that only the fundamental frequency is explicitly present in the definition of the signal generator (43) and, hence, in the model reduced by moment-matching defined in equation (44), the mapping Ω^k is, effectively, polynomial (*i.e.* no fractional exponents of ξ are required for the regular wave input case).

As an initial assessment of this case study, Figure 3 illustrates the performance of a nonlinear moment-based reduced model as in equation (44), computed

with $k = 3$ (*i.e.* with Ω^k including three harmonics of the fundamental frequency ω^*). In particular, Figure 3 shows both the output of the target (dashed) nonlinear model of the WEC system (11), computed with a Runge-Kutta method (time-step[19] of 10^{-4} [s]), where the non-parametric convolution operator is explicitly solved, and the output of the moment-based reduced order model (44) (solid), with $k = 3$.

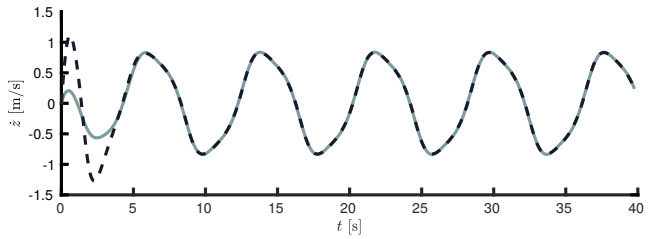

Fig. 3 Output of both the target nonlinear model (dashed) and the moment-based reduced order model (solid), with $k = 3$.

It can be readily appreciated that, after the corresponding transient period, the steady-state response of both target and approximating models are effectively indistinguishable, by virtue of the inherent moment-matching feature of the reduced model. To illustrate the improvement in (steady-state) accuracy for higher values of k, Figure 4 shows (in logarithmic scale) the absolute value of the difference between target and approximating output for $k \in \{3, 5, 7\}$, as a function of time. In addition, the error corresponding with the output of the system arising from Jacobian linearisation, *i.e.* the linear Cummins' equation in (20) (which naturally does not include any information regarding the nonlinear mapping f_{nl}), corresponding with the spherical heaving point absorber considered in this section, is also shown. Although, as can be concluded from both Figures 3 and 4, selecting $k = 3$ provides accurate results, these can be improved by increasing k accordingly.

Aiming to provide a conclusive performance indicator for this regular deterministic wave input case, the normalised mean absolute percentage error (NMAPE) is considered, defined as

$$\text{NMAPE}(\tilde{y}_{\text{ss}}) = \frac{100}{N_s} \sum_{i=1}^{N_s} \frac{|\tilde{y}_{\text{ss}}(t_i) - y_{\text{ss}}(t_i)|}{\max\{|y_{\text{ss}}(t_i)|\}}, \tag{45}$$

where $N_s \in \mathbb{N}_{\geq 1}$ denotes the number of (time-domain) samples available for the time-traces of the steady-state target, and approximating output signals y_{ss} and $\tilde{y}_{\text{ss}}$, respectively. Table 1 shows the NMAPE for the nonlinear moment-based models computed from equation (44), with $k \in \{3, 5, 7\}$, and that corresponding with the Jacobian linearisation about the origin, *i.e.* equation (20). Clearly, a result consistent with that shown in Figure 4 can be straightforwardly concluded.

# of harmonics	NMAPE
(Jacobian linearisation)	10.12 %
$k = 3$	0.76 %
$k = 5$	0.14 %
$k = 7$	0.04 %

Table 1 NMAPE for the moment-based reduction strategy, for WECs under regular excitation.

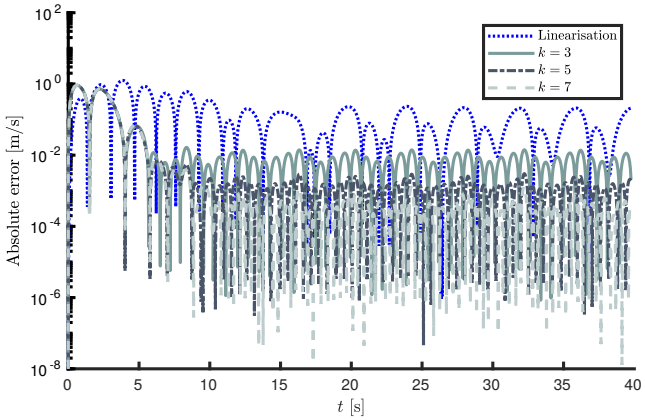

Fig. 4 Absolute value of the difference between target and approximating output for $k \in \{3, 5, 7\}$, as a function of time. In addition, the error corresponding with the output of the Jacobian linearisation is also shown.

7.2 Stochastic regular excitation

Section 7.1 discusses a case study where the amplitude associated with the regular wave excitation input f_{e} is exactly known. In other words, a single trajectory $\xi(t)$ of the signal generator (43), obtained from a unique initial condition $\xi(0)$, is required to fully characterise the approximating moment $h \circ \tilde{\pi}$, in terms of the Galerkin-like approach presented in Section 5.1. If the wave height, characterising the wave excitation amplitude, is only known to lie within a certain set, *i.e.* $H_w \in \mathscr{H}$, with $\mathscr{H} = [H_w^{\min}, H_w^{\max}] \subset \mathbb{R}^+$, then the approximation of the corresponding nonlinear moment depends on an *infinite* number of initial conditions (each for every possible wave height in the set $\mathscr{H}$). Note that

[19] A small time-step is selected (with respect to the dominant system dynamics) to guarantee convergence in the benchmark response.

this stochastic regular wave case is used as a 'stepping stone' for the methodology proposed in the fully stochastic irregular input case, developed in Section 8.

Though an adaptation of the Galerkin-like approach, proposed in Section 5.1, is given in Section 6.2 for the multiple trajectory case, the number of initial conditions is assumed to be finite. Motivated by this, a *worst-case approach*[20] is considered in the following: Only the set of initial conditions $\Xi_t = \{\zeta^{\min}, \zeta^{\max}\} \subset \mathbb{R}^2$ are taken into account for the computation of the matrix $\tilde{\Pi}$, where $\zeta^{\min}$ and $\zeta^{\max}$ correspond with the inputs with height $H_w^{\min}$ and $H_w^{\max}$, respectively.

Remark 25 From now on, the elements of the set of initial conditions Ξ_t, associated with the worst-case approach described in this section, are referred to as *training initial conditions*. Analogously, the trajectories generated as a function of the set Ξ_t, *i.e.* $\{\xi_{\zeta^{\min}}, \xi_{\zeta^{\max}}\}$, are referred to as *training trajectories*.

Note that the set of training initial conditions can be computed analogously to equation (42), *i.e.*

$$\begin{aligned} \zeta^{\min} &= \begin{bmatrix} \frac{A_1^*}{2} & \frac{A_1^*}{2} \end{bmatrix}^\intercal, \quad A_1^* = |K_e(\omega^*)| \frac{H_w^{\min}}{2}, \\ \zeta^{\max} &= \begin{bmatrix} \frac{A_2^*}{2} & \frac{A_2^*}{2} \end{bmatrix}^\intercal, \quad A_2^* = |K_e(\omega^*)| \frac{H_w^{\max}}{2}. \end{aligned} \tag{46}$$

For this case study, it is assumed that $H_w^{\min} = 1.6$ [m] and $H_w^{\max} = 2.4$ [m], *i.e.* the actual value of the wave height can vary $\pm$ 20% of the nominal value $H_w = 2$ [m], adopted in Section 7.1. The approximating moment is then computed as detailed in Section 6.2, for the set of training trajectories Ξ_t, and where, in the light of the results computed for the deterministic case of Section 7.1, the number of harmonics involved in the definition of Ω^k is set to $k = 5$. Figure 5 illustrates the output of the nonlinear moment-based reduced order model (in steady-state, solid), for the inputs corresponding with the training trajectories $\xi_{\zeta^{\min}}$ and $\xi_{\zeta^{\max}}$. The target outputs, computed from system Σ in (11) using a Runge-Kutta method with a time-step of 10^{-4} [s] (as in Section 7.1), are denoted with a dashed line.

Remark 26 Note that, as expected from the method proposed in Section 6.1, the performance of the approximating outputs for the training trajectories $\xi_{\zeta^{\min}}$ and $\xi_{\zeta^{\max}}$, is not as accurate as in the deterministic case presented in Section 7.1. In particular, the latter is fully characterised by a single trajectory ξ, and the approximating moment can be computed with the Galerkin-like approach proposed in this paper, with an arbitrary degree of precision (facilitated by an appropriate selection of k in the mapping Ω^k). When multiple trajectories for the signal generator (S, L) are considered, a minimisation approach is utilised, where a single matrix $\tilde{\Pi}$ is computed to characterise the approximating moment $h \circ \tilde{\pi}$ for *all* the training trajectories involved, hence providing a more versatile reduced order model (*i.e.* valid for a larger class of inputs) but, naturally, with a corresponding loss in performance.

[20] The approach presented herein is simply one possibility: The user is free to select a finite set of initial conditions using different methods, according to specific application requirements.

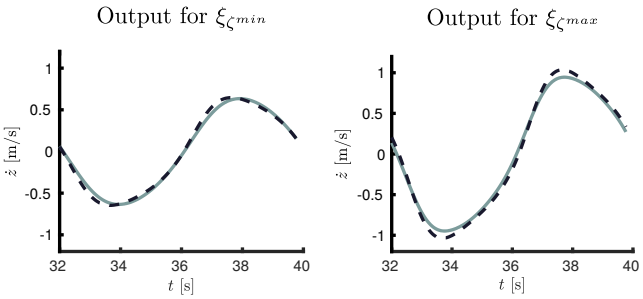

Fig. 5 Output of the nonlinear moment-based reduced order model (in steady-state, solid), for the inputs corresponding with the training trajectories $\xi_{\zeta^{\min}}$ and $\xi_{\zeta^{\max}}$. The target outputs are denoted with a dashed line.

To illustrate the performance of the moment-based reduced model computed in this section, a set of 1000 randomly generated realisations of regular wave inputs with wave heights in the set $[1.6, 2.4]$ [m], is considered. In particular, Figure 6 shows the NMAPE (computed as in equation (45)) for each wave realisation involved. Note that the average NMAPE value is $\overline{\text{NMAPE}} \approx 3\%$, and the maximum error registered is of $\approx 4\%$. In other words, using the methodology proposed in this section for the selection of an appropriate set of training trajectories to compute the approximating moment, the reduced order model by moment-matching (44) is able to successfully approximate the behaviour of the target non-parametric WEC system Σ, for regular wave excitation inputs with varying (stochastic) wave height.

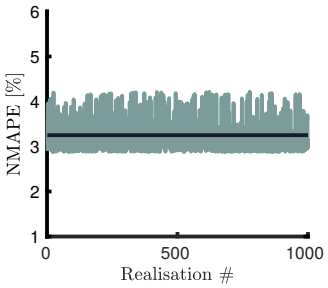

Fig. 6 NMAPE for 1000 realisations of regular wave inputs with $H_w \in [1.6, 2.4]$ [m]. The average value $\overline{\text{NMAPE}} \approx 3\%$ is denoted with a horizontal black line.

8 WEC systems under irregular wave excitation

The case of model order reduction by moment-matching for irregular sea states has a number of distinctive features with respect to the regular wave excitation cases discussed in Section 7, which, unless addressed appropriately, can substantially compromise the synthesis of such a nonlinear reduced structure. To be precise, irregular ocean waves are commonly represented in terms of a stochastic model: given a fixed location in space, the time series of a wave corresponds with a spectral density function (SDF) $S_w : \mathbb{R} \to \mathbb{R}$, $\omega \mapsto S_w(\omega)$, characterising (stochastically) the behaviour of ocean waves at this specific location. Examples of widely-used (semi-empirical) SDFs are the JONSWAP spectrum [19], for wind-generated seas with fetch limitations, the Bretschneider spectrum [5] for developing seas, and the Pierson-Moskowitz spectrum [31], for fully-developed seas.

That said, in this irregular wave input scenario, height and period are not exactly known, but only knowledge of the so-called significant wave height $\bar{H}_w$ and peak period $\bar{T}_w$ are commonly available, for a given stochastic sea-state characterisation in terms of a particular SDF. This clearly has several implications, both on the definition of the signal generator characterising the wave excitation effect (as in equation (16)), and the methodology involved in the computation of the approximating moment. These implications are addressed and discussed in the following subsections.

8.1 On the definition of the signal generator

Recall that the signal generator (16) is composed of $\mathbf{f}$ harmonics of a fundamental frequency ω_0, *i.e.* the set $\mathscr{F} = \{h_p\omega_0\}_{p=1}^{\mathbf{f}}$, with $\mathcal{H} = \{h_p\}_{p=1}^{\mathbf{f}} \subset \mathbb{N}_{\geq 1}$, and where $h_1 < \ldots < h_{\mathbf{f}}$. Though this assumption is, in principle, not restrictive (see [24]), an accurate representation of wave excitation effects potentially requires both a *sufficiently small* fundamental frequency ω_0, and a *sufficiently large* number of harmonics $\mathbf{f}$. This, in turn, has the following consequences:

1) A small fundamental frequency implies that the projection, involved in the Galerkin-like procedure proposed to compute the approximating moment, has to be performed on a larger time interval $\mathcal{T} = [0, 2\pi/\omega_0]$. Though this can be still performed efficiently using FFTs (see Section 6), it can also increase the computational complexity involved in the solution of the projected residual equation (34).
2) A large number of harmonics $\mathbf{f}$ in the definition of the signal generator (16) directly affects the complexity of the resulting reduced model by moment-matching: the order (dimension) ν of the family of reduced order models achieving moment-matching (32) depends linearly on $\mathbf{f}$.

The issue discussed in item 1) above, can be easily overcome by a sensible selection of the fundamental frequency, which should take into account the particular sea state under analysis (further discussed in the case study provided in this section). Item 2) above can be overcome in the spirit of the linear moment-based technique for WECs proposed in [9, 28]: Only a set of *dynamically relevant* frequencies should be selected to represent the wave excitation effects and, hence, to characterise the corresponding reduced order model by moment-matching. As demonstrated in [9,28], this set, for the WEC case, includes the resonant frequency associated with the linearised behaviour of the WEC system (*i.e.* the frequency characterising the H_∞-norm of the linearised system, see [44]), and the peak frequency characterising the input SDF, *i.e.* $\bar{\omega}_w = 2\pi/\bar{T}_w$.

8.2 On the definition of the set of training trajectories

Given the stochastic nature of the wave process, and once the set of frequencies $\mathscr{F}$ involved in the definition of the corresponding signal generator is selected (following Section 8.1), a method to choose a set of training trajectories is required, similarly to the case discussed in Section 7.2.

Inspired by the worst-case approach defined for the case of regular wave excitation with stochastic height, the following procedure is proposed. Recall that every initial condition $\xi(0)$ can be written as in Remark 9, *i.e.* in terms of a set of coefficients $\{\alpha_p, \beta_p\}_{i=1}^{f} \subset \mathbb{R}$, associated to each harmonic $h_p\omega_0$ involved in the definition of the signal generator. Let $A_p = \sqrt{\alpha_p^2 + \beta_p^2} \in \mathbb{R}^+$, with $p \in \mathbb{N}_{\mathbf{f}}$, be a set of positive real-valued 'amplitudes' associated with[21] each harmonic h_p. Then:

- Generate a random set of $N_t \in \mathbb{N}_{\geq 1}$ initial conditions $\Xi = \{\zeta_i\}_{i=1}^{N_t}$ (*i.e.* wave inputs), according to the SDF S_w characterising the sea state under analysis.
- Compute the set $\mathscr{A}_p = \{A_p^i\}_{i=1}^{N_t}$, with $p \in \mathbb{N}_{\mathbf{f}}$, for each randomly generated initial condition ζ_i, where A_p^i denotes the amplitude associated with the harmonic $h_p\omega_0$.
- Select the set of initial conditions Ξ_t that maximise and minimise each $\mathscr{A}_p$, denoted as $\zeta_p^{\min}$ and $\zeta_p^{\max}$, for every $p \in \mathbb{N}_{\mathbf{f}}$. Note that this automatically implies

[21] The use of the term 'amplitude' for A_p is justified in Remark 27.

that $2\mathbf{f}$ initial conditions are selected (one amplitude maximiser and one minimiser for each harmonic h_p involved in the definition of the signal generator).
- Compute the set of *training trajectories* using Ξ_t, directly from the definition of the signal generator (15), *i.e.* the set $\{\xi_{\zeta_p^{\min}}, \xi_{\zeta_p^{\max}}\}_{p=1}^{\mathbf{f}}$.

Remark 27 The method proposed in this section is indeed analogous to the worst-case approach proposed in Section 7.2: Note that the value $A_p = \sqrt{\alpha_p^2 + \beta_p^2}$ corresponds to the absolute value of the complex number $(\alpha_p + j\beta_p)e^{h_p\omega_0 t}$, which characterises the entries of the trajectory $\xi(t)$ associated with the harmonic $h_p\omega_0$ (see Remark 9). In other words, the method outlined in this section retains, as training trajectories, only those trajectories associated with the maximum and minimum input amplitudes, for each harmonic $h_p\omega_0$, with $p \in \mathbb{N}_{\mathbf{f}}$.

8.3 Numerical study

For the remainder of this numerical study of nonlinear model reduction by moment-matching, under irregular wave excitation, an array of two identical spherical heaving point absorber WECs is considered, each device with a radius of 2.5 [m] (as in Section 7), in the layout configuration presented in Figure 7. The distance between devices is set to one diameter, *i.e.* $d = 5$ [m].

The nonlinear mapping f_{nl}, characterising the nonlinear effects for this WEC system, is given by:

$$f_{\text{nl}}(z, \dot{z}) = \begin{bmatrix} f_{\text{re}}^{\text{nl}}(z_1) + f_v(\dot{z}_1) \\ f_{\text{re}}^{\text{nl}}(z_2) + f_v(\dot{z}_2) \end{bmatrix}, \tag{47}$$

where the mappings $f_{\text{re}}^{\text{nl}}$ and f_v are defined as in equation (41), and where $z_1 : \mathbb{R}^+ \to \mathbb{R}$ and $z_2 : \mathbb{R}^+ \to \mathbb{R}$ denote the displacement of device 1 and 2, respectively.

Remark 28 Note that the WEC system, presented in the layout of Figure 7, can be regarded as a single-input system: Given the direction of the incident waves, and the underlying symmetry of the layout, the wave excitation force experienced by both devices is indeed the same. In other words, the single-output signal generator defined in equation (15) can be utilised to describe f_{e}. In addition, from now on, the velocity of device 1, *i.e.* $\dot{z}_1$, is selected as target output[22].

The numerical generation of the irregular input waves, for this case study, is fully characterised by a JONSWAP spectrum with $\bar{H}_w = 2$ [m] and $\bar{T}_w = 8$ [s]. The so-called peak enhancement factor [19] is set to $\gamma = 3.3$. The corresponding SDF S_w is that illustrated in Figure 8.

[22] This is considered to simplify the case study, and focus on the performance of the nonlinear reduction technique.

Following Section 8.1, and given the specific SDF selected for the generation of numerical waves, the fundamental frequency is set to a value of $\omega_0 = 0.1$ [rad/s], which facilitates a sufficiently accurate representation of the wave process for the synthesis of the corresponding reduced order model, as demonstrated in the remainder of this section. In addition, the signal generator involved in the definition of the reduced model by moment-matching, *i.e.* equation (15), is characterised with the set of frequencies $\mathscr{F} = \{0.8, 2\}$, where, given the selection of $\omega_0 = 0.1$ [rad/s], the set $\mathcal{H} = \{h_1, h_2\} = \{8, 20\}$.

Remark 29 Note that, as discussed in Section 8.1, the selection of the set $\mathscr{F}$ is not arbitrary: 0.8 [rad/s] represents the frequency corresponding with the peak characterising the wave input SDF (see Figure 8), while 2 [rad/s] is the frequency characterising the $\mathscr{H}_\infty$-norm of the Jacobian linearisation of the WEC system, *i.e.* the resonant frequency corresponding to heave motion.

Remark 30 With the selection of frequencies in the set $\mathscr{F}$, the order (dimension) of the reduced model by moment-matching (as in equation (32)) is $\nu = 2\mathbf{f} = 4$.

Remark 31 The generation of waves for the assessment of the proposed strategy, *i.e.* in the simulation stage, is naturally performed using both a smaller value of ω_0, and a higher number of harmonics, than those specified in the signal generator used to synthesise the moment-based reduced model. This is specified and detailed in the following paragraphs.

Once the set $\mathscr{F}$ is defined, the set of training trajectories, utilised to compute an approximation of the moment of the WEC system at the signal generator (S, L), is obtained following Section 8.2. In particular, a set of $N_t = 50$ random initial conditions is considered[23] to compute the sets $\mathscr{A}_1 = \{A_1^i\}_{i=1}^{50}$ and $\mathscr{A}_2 = \{A_2^i\}_{i=1}^{50}$, associated with the harmonics corresponding with $h_1 = 8$ (0.8 [rad/s]) and $h_2 = 20$ (2 [rad/s]), respectively. These sets are illustrated in Figure 9, where the maximum and minimum values for each set $\mathscr{A}$ are denoted using the black color.

With the result presented in Figure 9, one can completely characterise the set of training trajectories , *i.e.* the set of trajectories $\{\xi_{\zeta_1^{\min}}, \xi_{\zeta_1^{\max}}, \xi_{\zeta_2^{\min}}, \xi_{\zeta_2^{\max}}\} \subset \mathbb{R}^4$. Finally, aiming to retain the output mapping, characterising the reduced model by moment-matching, in a polynomial form (analogously to the case of regular input waves discussed in Section 7), the mapping Ω^k, utilised to compute the approximating moment $h \circ \tilde{\pi}$, is chosen as described in Section 22. In particular, the

[23] Computed randomly according to the SDF of Figure 8.

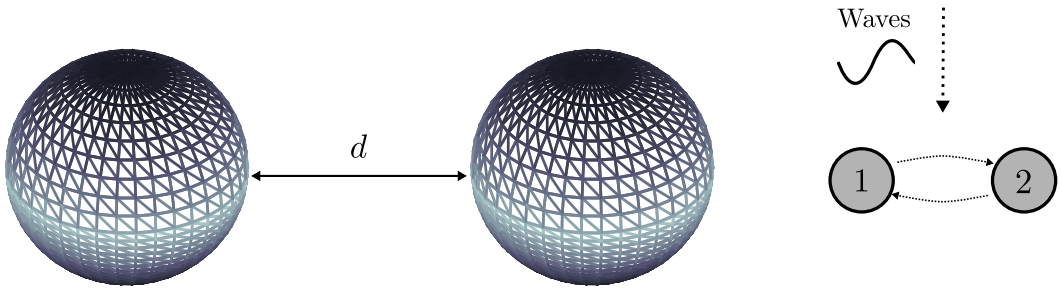

Fig. 7 Spherical heaving point absorber WEC layout considered for the case of nonlinear model reduction under irregular wave excitation.

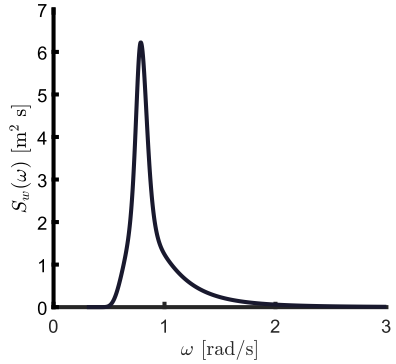

Fig. 8 SDF corresponding with a JONSWAP spectrum utilised to generate the wave input.

maximum number of harmonics associated with each frequency in the set $\mathscr{F}$ is set to $k_1^{\max} = 5$ and $k_2^{\max} = 3$, *i.e.* 5 and 3 harmonics associated with the frequencies 0.8 [rad/s] and 2 [rad/s], respectively. Analogously to the regular input case with stochastic height of Figure 5, the steady-state output of the nonlinear moment-based reduced order model computed in this section, for the inputs corresponding with each training trajectory, is shown in Figure 10 (solid). The target outputs, for each corresponding training trajectory, are computed from the non-parametric WEC system Σ (as in equation (11)), with a Runge-Kutta method (time-step of 10^{-4} [s]), and can be appreciated in Figure 10 with dashed lines.

To begin with the assessment of the resulting reduced order model by moment-matching, Figure 11 presents results for a particular (randomly generated[24]) sea state realisation, where the input waves, considered for this simulation stage, are computed using a fundamental frequency $\omega_0 = 0.01$ [rad/s] and 400 harmonics (*i.e.* with a so-called *cut-off* frequency of 4 [rad/s]). As can be directly appreciated from Figure 11, the output of the reduced order model by moment-matching (solid) is effectively able to approximate the target output (dashed), even during the transient period. Note that the output corresponding with the Jacobian linearisation about the origin, *i.e.* linear Cummins' equation (20) for the analysed WEC system, is also shown, using a dotted line. A significant overprediction of velocity can be appreciated by the linear model, potentially leading to an overprediction of power production. The NMAPE, computed as in equation (45) for 100 [s] of simulation time (as shown in Figure 11), is $\approx 4.6\%$ for the nonlinear reduced model computed in this section, and $\approx 40\%$ for the case of the Jacobian linearisation.

A more detailed characterisation of the approximation error can be appreciated in Figure 12, where the absolute value of the difference between target and approximating output is shown, for both the reduced model by moment-matching, and the output arising from Jacobian linearisation.

To provide a conclusive illustration of the capabilities and performance of the moment-based model, the NMAPE for a set of 100 random realisations of wave inputs, according to the JONSWAP spectrum considered (see Figure 8), is explicitly shown in Figure 13. Note that the mean NMAPE is $\overline{\text{NMAPE}} \approx 4.5\%$, with any individual errors always below 6%, effectively showing the capabilities of the moment-based strategy, presented in this paper, to approximate the behaviour of a nonlinear WEC system under stochastic irregular wave excitation.

Remark 32 (On potential changes in the sea-state description) Note that, in general, there is no guarantee that a reduced model computed according to a specific sea-state description is still representative in a different input condition. While it is expected that the reduced structure is well-behaved for reasonable small variations in the nature of the sea-state, the user is recommended to re-compute a reduced model in such a situation, according to the updated input description.

Finally, and aiming to assess the computational features of the nonlinear moment-based reduced model computed in this section, Figure 14 shows:

[24] The methodology employed herein uses random amplitudes. The reader is referred to [24] for further detail.

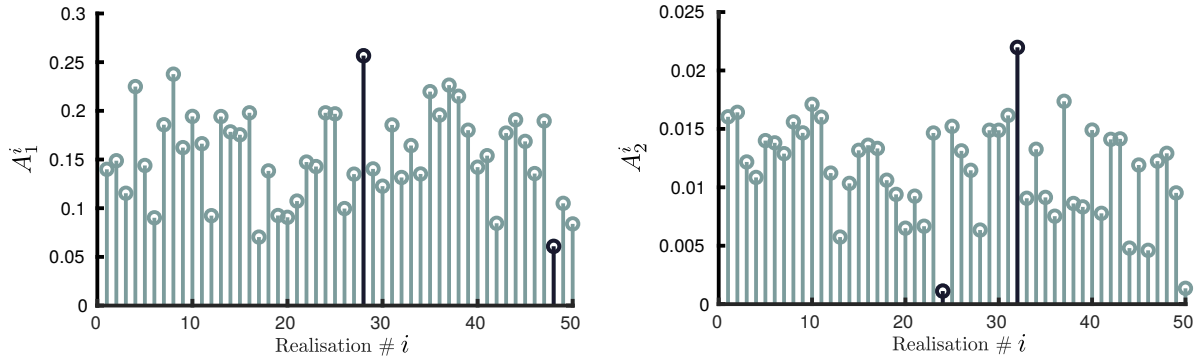

Fig. 9 Sets of amplitudes $\mathscr{A}_1 = \{A_1^i\}_{i=1}^{50}$ and $\mathscr{A}_2 = \{A_2^i\}_{i=1}^{50}$, associated with the harmonics corresponding with $h_1 = 8$ and $h_2 = 20$, respectively.

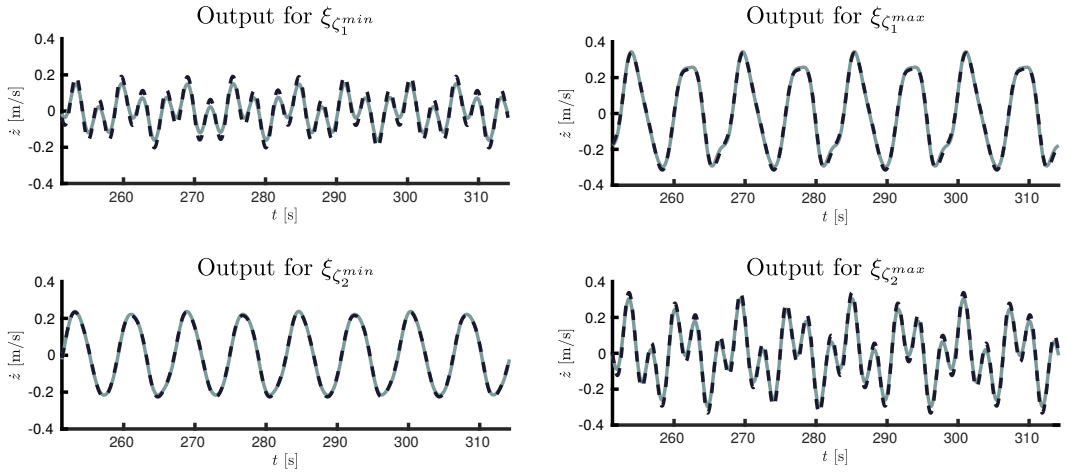

Fig. 10 Output of the nonlinear moment-based reduced order model under irregular wave excitation (in steady-state, solid), for the inputs corresponding with each training trajectory. The target outputs are denoted with a dashed line.

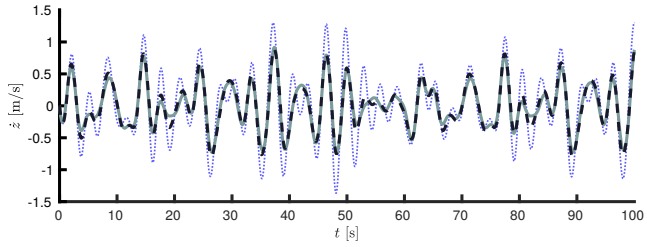

Fig. 11 Output of the reduced order model by moment-matching (solid) and target motion (dashed), for a randomly generated sea-state realisation, with SDF as in Figure 8. The output corresponding with the Jacobian linearisation about the origin is also shown, using a dotted blue line.

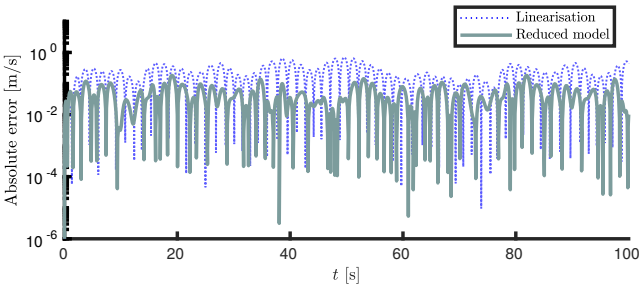

Fig. 12 Absolute value of the difference between target and approximating output, for the case of irregular wave excitation. The error corresponding with the output of the Jacobian linearisation is also shown.

A) Normalised run-time[25] for a parametric nonlinear model of the WEC system, where the convolution operation associated with radiation forces is replaced with a reduced order model (in state-space) of order 8, following the *linear* moment-based strategy presented in [9] using the same frequency interpolation set considered in this section, *i.e.* $\mathscr{F} = \{0.8, 2\}$ [rad/s].

B) Normalised run-time for the nonlinear reduced model by moment-matching computed as detailed in this section.

[25] Ratio between the time required to compute the output of each corresponding model, and the length of the simulation itself. The computations are performed using Matlab®, running on a PC composed of an Intel Core i7-5550U processor with 8GB of RAM.

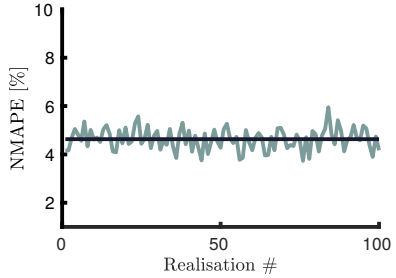

Fig. 13 NMAPE for 100 realisations of irregular wave inputs according to the SDF presented in Figure 8. The average value $\overline{\text{NMAPE}} \approx 4.5\%$ is denoted with a horizontal black line.

Remark 33 Note that for case A), detailed above, no 'nonlinear model reduction' takes place, but only the *linear* convolution term is replaced with a state-space form to alleviate the computational requirements of the convolution itself (see also Remark 1).

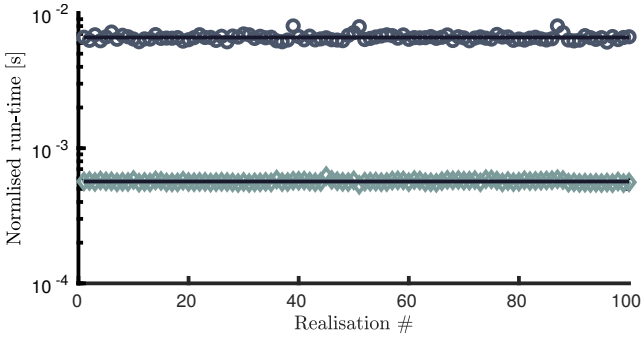

Fig. 14 Normalised run-time for a parametric nonlinear model of the WEC system (circles, upper trace), where the convolution operation is replaced with a reduced order model (in state-space), and for the nonlinear reduced model by moment-matching computed as detailed in this section (diamonds, lower trace). Mean values are indicated with black horizontal lines.

It can be readily appreciated that the reduced nonlinear model, presented in this paper, computes in an order of magnitude faster than the original parametric model, which can be attributed to two main features. Firstly, a smaller order (dimension) is required to represent the behaviour of the WEC system, which effectively leads to faster computations. Secondly, and more importantly, the input-to-state dynamics are *linear*, and only the output mapping presents nonlinear behaviour (which is *static*). In other words, the main computational cost behind the moment-based reduced model is simply solving a set of first order *linear* ordinary differential equations. This feature is indeed appealing from a control/state-estimation perspective, where both efficient and precise models are required.

9 Conclusions

This paper presents a nonlinear model reduction framework for wave energy applications, based on moment-matching techniques, which inherently preserve steady-state response characteristics. This is, to the best of the authors' knowledge, the first truly systematic nonlinear model reduction technique proposed in the wave energy field. The first contribution of this study concerns the proof of existence and uniqueness of the corresponding nonlinear moment for the non-parametric WEC system Σ. Secondly, and given the intrinsic necessity of an analytic expression for the corresponding nonlinear moment, a consistent approximation method is presented, by a suitably defined family of functions, in terms of a Galerkin-like methodology. Practical aspects behind this approximation framework are given and discussed, including the connection (and use) of well-established algorithms, to efficiently compute such an approximating moment.

The family of nonlinear models reduced by moment-matching proposed in this paper is inherently parametric (given specifically in state-space form), and input-to-state *linear*, with any nonlinear behaviour confined to the output mapping only. Moreover, given the nature of the Galerkin-like method proposed to approximate the corresponding moment, the user can manipulate the degree of complexity of this nonlinear output mapping, hence having full control of the underlying characteristics of the reduced structure, generating a continuum of models with varying NMAPE/complexity tradeoff.

Two different model reduction cases are clearly defined, in terms of the nature of the input: model reduction of nonlinear WEC systems under regular, and irregular, wave excitation. For WECs under regular wave excitation, both deterministic and stochastic wave height cases are considered. In the deterministic case, the wave height is assumed to be known, and the approximating moment can be characterised in terms of a single trajectory associated with the corresponding signal generator. For the stochastic case, the wave height is only assumed to lie within a certain (given) set, which directly implies that, in principle, an infinite number of inputs needs to be considered within the approximation process. In the light of this, a worst-case approach is proposed to select a finite set of so-called training trajectories, representing the 'limit' cases associated with the set of heights. Case studies are presented for both deterministic and stochastic cases, in terms of a spherical heaving point absorber WEC, including both nonlinear viscous, and hydrostatic restoring effects. It is shown that the nonlinear models reduced by moment-matching, can successfully approximate the nonlinear

target WEC system Σ, with a NMAPE always below 4%, clearly showing the capabilities of the strategy.

For the case of irregular waves, given the (fully) stochastic nature of the wave input, methods are provided to select the characteristics describing the wave excitation effects, both in terms of the fundamental frequency, and the harmonics required in the definition of the signal generator. In addition, and analogously to the stochastic regular input case, a methodology to select a set of training trajectories is provided, also based on a worst-case approach. A numerical case study is provided, considering a WEC system composed of two heaving point absorber devices, presenting nonlinear behaviour (nonlinear viscous and hydrostatic restoring effects). The average NMAPE for this case study is $\approx 4.5\%$, effectively showing the capabilities of the proposed moment-based strategy to approximate the behaviour of a nonlinear WEC system under stochastic irregular wave excitation. Finally, a study on the normalised run-time is provided, showing that the presented strategy computes in an order of magnitude less than when solving the nonlinear Cummins' equation (11) with a state-space description approximating the non-parametric (convolution) terms. This significant reduction in computational complexity, for modest NMAPE values, gives the obtained models capabilities to be used in design and synthesis of real-time WEC controllers, hence directly contributing in the roadmap towards WEC commercialisation.

Acknowledgements This work was supported by the Science Foundation Ireland under Grant No. SFI/13/IA/1886. The authors are grateful with Prof. Alessandro Astolfi and Dr. Giordano Scarciotti from the Control and Power Group, Imperial College London, for useful discussions on nonlinear moment-based theory.

Conflict of interest

The authors declare that they have no conflict of interest.

References

1. Astolfi, A.: Model reduction by moment matching for linear and nonlinear systems. IEEE Transactions on Automatic Control **55**(10), 2321–2336 (2010)
2. Aubin, J.P.: Applied functional analysis, vol. 47. John Wiley & Sons (2011)
3. Bacelli, G., Genest, R., Ringwood, J.V.: Nonlinear control of flap-type wave energy converter with a non-ideal power take-off system. Annual Reviews in Control **40**, 116–126 (2015)
4. Boyd, J.P.: Chebyshev and Fourier spectral methods. Courier Corporation (2001)
5. Bretschneider, C.L.: Wave variability and wave spectra for wind-generated gravity waves. Tech. Rep. 118, Beach Erosion Board, US Army, Corps of Engineers (1959)
6. Coleman, T.F., Li, Y.: An interior trust region approach for nonlinear minimization subject to bounds. SIAM Journal on optimization **6**(2), 418–445 (1996)
7. Cummins, W.: The impulse response function and ship motions. Tech. rep., DTIC Document (1962)
8. Faedo, N., Olaya, S., Ringwood, J.V.: Optimal control, MPC and MPC-like algorithms for wave energy systems: An overview. IFAC Journal of Systems and Control **1**, 37–56 (2017)
9. Faedo, N., Peña-Sanchez, Y., Ringwood, J.V.: Finite-order hydrodynamic model determination for wave energy applications using moment-matching. Ocean Engineering **163**, 251 – 263 (2018)
10. Faedo, N., Peña-Sanchez, Y., Ringwood, J.V.: Parametric representation of arrays of wave energy converters for motion simulation and unknown input estimation: A moment-based approach. Applied Ocean Research **98**, 102055 (2020)
11. Faedo, N., Scarciotti, G., Astolfi, A., Ringwood, J.V.: Moment-based constrained optimal control of an array of wave energy converters. In: 2019 American Control Conference (ACC), Philadelphia, pp. 4797–4802 (2019)
12. Faedo, N., Scarciotti, G., Astolfi, A., Ringwood, J.V.: Nonlinear energy-maximising optimal control of wave energy systems: A moment-based approach. IEEE Transactions on Control Systems Technology (under review) (2020)
13. Falnes, J.: Ocean waves and oscillating systems: linear interactions including wave-energy extraction. Cambridge university press (2002)
14. Finlayson, B., Scriven, L.: The method of weighted residualsa review. Appl. Mech. Rev **19**(9), 735–748 (1966)
15. Garcia-Rosa, P.B., Lizarralde, F., Estefen, S.F.: Optimization of the wave energy absorption in oscillating-body systems using extremum seeking approach. In: 2012 American Control Conference (ACC), pp. 1011–1016. IEEE (2012)
16. Giorgi, G.: Nonlinear hydrodynamic modelling of wave energy converters under controlled conditions. Ph.D. thesis, Department of Electronic Engineering, Maynooth University (2018)
17. Giorgi, G., Gomes, R.P.F., Bracco, G., Mattiazzo, G.: Numerical investigation of parametric resonance due to hydrodynamic coupling in a realistic wave energy converter. Nonlinear Dynamics (2020)
18. Giorgi, G., Ringwood, J.V.: Consistency of viscous drag identification tests for wave energy applications. In: Proceedings of the 12th European Wave and Tidal Energy Conference (EWTEC). Cork (2017)
19. Hasselmann, K.: Measurements of wind wave growth and swell decay during the Joint North Sea Wave Project (JONSWAP). Dtsch. Hydrogr. Z. **8**, 95 (1973)
20. Isidori, A.: Nonlinear control systems. Springer Science & Business Media (2013)
21. Isidori, A., Astolfi, A.: Disturbance attenuation and h_∞-control via measurement feedback in nonlinear systems. IEEE transactions on automatic control **37**(9), 1283–1293 (1992)
22. Kautsky, J., Nichols, N.K., Van Dooren, P.: Robust pole assignment in linear state feedback. International Journal of control **41**(5), 1129–1155 (1985)
23. Korde, U.A., Ringwood, J.V.: Hydrodynamic control of wave energy devices. Cambridge University Press (2016)

24. Mérigaud, A., Ringwood, J.V.: Free-surface time-series generation for wave energy applications. IEEE Journal of Oceanic Engineering **43**(1), 19–35 (2018)
25. Nielsen, S.R., Zhou, Q., Kramer, M.M., Basu, B., Zhang, Z.: Optimal control of nonlinear wave energy point converters. Ocean engineering **72**, 176–187 (2013)
26. Padoan, A., Scarciotti, G., Astolfi, A.: A geometric characterization of the persistence of excitation condition for the solutions of autonomous systems. IEEE Transactions on Automatic Control **62**(11), 5666–5677 (2017)
27. Papillon, L., Costello, R., Ringwood, J.V.: Boundary element and integral methods in potential flow theory: a review with a focus on wave energy applications. Journal of Ocean Engineering and Marine Energy pp. 1–35 (2020)
28. Peña-Sanchez, Y., Faedo, N., Ringwood, J.V.: Moment-based parametric identification of arrays of wave energy converters. In: 2019 American Control Conference (ACC), pp. 4785–4790. IEEE (2019)
29. Penalba, M., Ringwood, J.V.: Linearisation-based nonlinearity measures for wave-to-wire models in wave energy. Ocean Engineering **171**, 496–504 (2019)
30. Penalba Retes, M., Ringwood, J.V.: Systematic complexity reduction of wave-to-wire models for wave energy system design. Ocean Engineering (accepted June 2020) (2020)
31. Pierson Jr, W.J., Moskowitz, L.: A proposed spectral form for fully developed wind seas based on the similarity theory of sa kitaigorodskii. Journal of geophysical research **69**(24), 5181–5190 (1964)
32. Rao, K.R., Kim, D.N., Hwang, J.J.: Fast Fourier transform-algorithms and applications. Springer Science & Business Media (2011)
33. Ringwood, J.V., Bacelli, G., Fusco, F.: Energy-maximizing control of wave-energy converters: The development of control system technology to optimize their operation. IEEE Control Systems **34**(5), 30–55 (2014)
34. Ruehl, K., Bull, D.: Wave Energy Development Roadmap: Design to commercialization. OCEANS 2012 MTS/IEEE: Harnessing the Power of the Ocean (2012)
35. Scarciotti, G., Astolfi, A.: Data-driven model reduction by moment matching for linear and nonlinear systems. Automatica **79**, 340–351 (2017)
36. Scarciotti, G., Astolfi, A.: Nonlinear model reduction by moment matching. Foundations and Trends in Systems and Control **4**(3-4), 224–409 (2017)
37. Scruggs, J., Lattanzio, S., Taflanidis, A., Cassidy, I.: Optimal causal control of a wave energy converter in a random sea. Applied Ocean Research **42**, 1–15 (2013)
38. Suchithra, R., Ezhilsabareesh, K., Samad, A.: Development of a reduced order wave to wire model of an owc wave energy converter for control system analysis. Ocean Engineering **172**, 614–628 (2019)
39. Sun, Z., Zhao, A., Zhu, L., Lu, K., Wu, W., Blaabjerg, F.: Extremum-seeking control of wave energy converters using two-objective flower pollination algorithm. In: 2018 IEEE International Power Electronics and Application Conference and Exposition (PEAC), pp. 1–5. IEEE (2018)
40. Taghipour, R., Perez, T., Moan, T.: Hybrid frequency–time domain models for dynamic response analysis of marine structures. Ocean Engineering **35**(7), 685–705 (2008)
41. Urabe, M.: Galerkin's procedure for nonlinear periodic systems. Archive for Rational Mechanics and Analysis **20**(2), 120–152 (1965)
42. Wazwaz, A.M.: Volterra integro-differential equations. In: Linear and Nonlinear Integral Equations, pp. 175–212. Springer (2011)
43. Wendt, F., Nielsen, K., Yu, Y.H., Bingham, H., Eskilsson, C., Kramer, M., Babarit, A., Bunnik, T., Costello, R., Crowley, S., et al.: Ocean energy systems wave energy modelling task: Modelling, verification and validation of wave energy converters. Journal of Marine Science and Engineering **7**(11), 379 (2019)
44. Zhou, K., Doyle, J.C.: Essentials of robust control, vol. 104. Prentice hall Upper Saddle River, NJ (1998)